siam

18th Annual Meeting of the Bulgarian Section of SIAM
December 11 – 13, 2022
Sofia

BGSIAM'23

EXTENDED ABSTRACTS

HOSTED BY THE JOINT INNOVATION CENTRE
BULGARIAN ACADEMY OF SCIENCES

18th Annual Meeting of the Bulgarian Section of SIAM
December 11 – 13, 2023, Sofia

BGSIAM'23 Extended abstracts

ISSN: 1314-7145 (electronic)

PREFACE

The Bulgarian Section of SIAM (BGSIAM) was formed in 2007 with the purpose to promote and support the application of mathematics to science, engineering and technology in Republic of Bulgaria. The goals of BGSIAM follow the general goals of SIAM:

- To advance the application of mathematics and computational science to engineering, industry, science, and society;
- To promote research that will lead to effective new mathematical and computational methods and techniques for science, engineering, industry, and society;
- To provide media for the exchange of information and ideas among mathematicians, engineers, and scientists.

During the BGSIAM'23 conference a wide range of problems concerning recent achievements in the field of industrial and applied mathematics will be presented and discussed. The meeting provides a forum for exchange of ideas between scientists, who develop and study mathematical methods and algorithms, and researchers, who apply them for solving real life problems.

The strongest research groups in Bulgaria in the field of industrial and applied mathematics, advanced computing, mathematical modelling and applications will be presented at the meeting according to the accepted extended abstracts. Many of the participants are young scientists and PhD students.

LIST OF INVITED SPEAKERS:

- Professor Daniel Dantchev (Institute of Mechanics, Bulgarian Academy of Sciences)
  "Fluctuation-induced Interactions in Micro- and Nano-systems: Survey of Analytical Results for Basic Models"
- Professor Radka Stoyanova (University of Miami Leonard M. Miller School of Medicine, USA)
  "Radiogenomic Characterization of MRI Habitats for Effective Management of Prostate Cancer"
- Dr. Daniela Doneva (Emmy Noether Research Group Leader at the University of Tübingen, Germany)
  "Numerical relativity simulations in theories beyond General Relativity"

The present volume contains extended abstracts of the presentations (Part A) and list of participants (Part B).

Assoc. Prof. Elena Lilkova
Chair of BGSIAM Section

Prof. Maria Datcheva
Vice-Chair of BGSIAM Section

Assoc. Prof. Todorka Alexandrova
Secretary of BGSIAM Section

Sofia, December 2023

Table of Contents

Part A
Extended abstracts[1]

[1] Arranged alphabetically according to the family name of the first author.

Numerical solution of space fractional diffusion equation using collocation method

H. Bansu, S. Margenov

Fractional order derivative provide more accurate models of the considered systems. In this paper, numerical technique of collocation is used to solve class of initial boundary value problems for the space fractional diffusion equations in finite domain. The fractional derivatives are considered in the Caputo sense. The proposed numerical approach approximates spatial direction using radial basis functions and temporal direction using Chebyshev polynomials. We have implemented Chebyshev discritization in space and uniform discritization in time direction. Also, the discretizations for space and time are independent of each other.
Moreover, numerical experiments are presented and the results are compared with the exact solution and also with the results obtained via other methods in the literature. The comparison reveals that the proposed method is more reliable and more accurate. The results are also analyzed under the influence of fractional derivative. The diffusion profiles are obtained along time and distance for different order of fractional derivatives in order to show the applicability of the proposed scheme.

Assessment of the Drought and Wetness Characteristics over Bulgaria by Means of the Standardized Precipitation Index

H. Chervenkov

Drought is a weather and climate-related phenomenon of complex nature which is a usual part of the climate practically of all parts of the world. It can significantly impact many vulnerable sectors due to its diversified geographical and temporal distribution. Relatively large areas of Europe, in particular Southeastern Europe including Bulgaria, have been affected by drought during the 20th century. Regardless of the type of the drought (meteorological, agricultural, hydrological, ground-water, streamflow, and socio-economic), the reduction in precipitation with respect to the normal precipitation amount is the primary driver, resulting in a successive shortage of water for different natural and human needs. Drought indices have been commonly used in climatology to define drought conditions and are, in general, functions of several hydro-meteorological variables. Among them the Standardized Precipitation Index (SPI) could be outlined due to its various strengths and, subsequently, it is worldwide increasingly used in both research and operational modes. The study presents an assessment of the drought and wetness characteristics of Bulgaria for the period 2014–2022 by means of this index calculated from precipitation data from more than 150 measurement stations. Figure 1 presents the time evolution of the field mean SPI-1/3/6 for the whole considered period. The relatively high number of stations ensures high land coverage and spatial representativeness. The rather big amount of data as well as the sophisticated calculation procedure of the

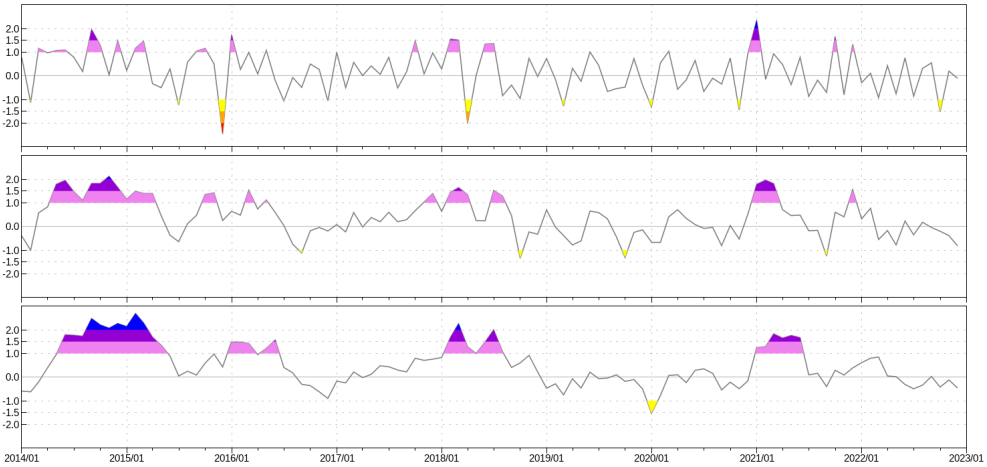

Figure 1: Time evolution of the field mean (over the territory of Bulgaria) SPI-1, SPI-3 and SPI-6 on the upper, middle and lower pane correspondingly

SPI (the computation of some special functions is needed) makes the considered problem computationally challenging.
Even though the considered period, at least from the point of view of regional climatology, is rather short, some relevant conclusions could be outdrawn from the study. First and foremost, it reveals the high spatial and temporal variability of the SPI which is a direct consequence of the spatial and temporal heterogeneity of the precipitation. Our findings show that several short-term droughts stand out, the more significant being in 2019–2020, but the wetness conditions generally prevail. The work could be extended and continued in many directions.
The results of the present study could be useful as a scientific basis for policy-making as well as an elaboration of drought consequence mitigation plans in various sensitive sectors.

Keywords: Drought Wetness, Precipitation Anomaly, Standardized Precipitation Index

Fluctuation-induced Interactions in Micro- and Nano-systems: Survey of Some Basic Results

D. Dantchev

The current review is based mainly on the following articles [1-3].
Fluctuations are ubiquitous: they unavoidably appear in any matter either due to its quantum nature or due to nonzero temperature of the material bodies and of the confined medium. If a material body is immersed in such a medium, its shape and the properties of its constituents modify the properties of the surrounding medium and its fluctuations. If in the same medium there is a second body then – in addition to all direct interactions between them – the

modifications due to the first body influence the modifications due to the second body. This mutual influence results in a *force* between these bodies, which goes under the general name of *fluctuation induced force*. If the excitations of the medium, which mediate the effective interaction between the bodies, are massless, this force is long-ranged and nowadays known as a *Casimir force*. If the fluctuating medium consists of a confined electromagnetic field in a vacuum, one speaks of the *quantum mechanical Casimir effect*. In the case that the order parameter of material fields fluctuates - such as differences of number densities or concentrations - and that the corresponding fluctuations of the order parameter are long-ranged, one speaks of the *critical Casimir effect*. This holds, e.g., in the case of systems which undergo a second-order phase transition and which are thermodynamically located near the corresponding critical point, or for systems with a broken continuous symmetry exhibiting Goldstone mode excitations. Here we review the currently available *exact results* concerning the critical Casimir effect in systems encompassing the one-dimensional Ising, XY, and Heisenberg models, the two-dimensional Ising model, the Gaussian and the spherical models, as well as the mean-field results for the Ising and the XY model. We present results both for the case of classical critical fluctuations if the system possesses a critical point at a non-zero temperature, as well as the case of quantum systems undergoing a continuous phase transition at zero temperature as a function of certain parameters. As confinements, we consider the film, the sphere-plane, and the sphere-sphere geometries. We discuss systems governed by short-ranged, by subleading long-ranged (i.e., of the van der Waals type), and by leading long-ranged interactions. In order to put the critical Casimir effect into the proper context and in order to make the review as self-contained as possible, basic facts about the theory of phase transitions, the theory of critical phenomena in classical and quantum systems, and finite-size scaling theory are recalled. Whenever possible, a discussion of the relevance of the exact results towards an understanding of available experiments is presented. The eventual applicability of the present results for certain devices is pointed out, too.

The strengths of the fluctuation-induced forces are proportional to the driving energy of the fluctuations, and thus to Planck's constant h in quantum systems and temperature T in classical systems.

When the degrees of freedom can enter and leave the region between the interacting objects one speaks about Casimir force. In the case of the electromagnetic Casimir force the medium is the vacuum, and the underlying mechanism is the set of quantum zero point or temperature fluctuations of the electromagnetic field. The now widely-investigated critical Casimir force (CCF) results from the fluctuations of an order parameter and more generally the thermodynamics of the medium supporting that order parameter in the vicinity of a critical point. Recently, a review on the exact results available for the CCF has been published in Ref. [1].

In recent Letter [2] we have introduced the terms of a Helmholtz fluctuation induced force. It is a force in which the order parameter value is fixed. We stress, that in customarily considered applications of, say, the equilibrium Ising model to binary alloys or binary liquids, if one insists on full rigor, the case with order parameter fixed must be addressed. In [2] via deriving there exact results on the example of Ising chain with fixed magnetization and under periodic boundary conditions, we have shown that the Helmholtz force has a behavior very different from that of the Casimir force. It is interesting to note that the studied Helmholtz force has a behavior similar to the one appearing in some versions of the big bang theory —

strong repulsion at high temperatures, transitioning to moderate attraction for intermediate values of the temperature, and then back to repulsion, albeit much weaker than during the initial period of highest temperature.
We stress that the definition and existence of Helmholtz force is by no means limited to the Ising chain and can be addressed, in principle, in any model of interest.
We note that the issue of the ensemble dependence of fluctuation-induced forces pertinent to the ensemble has yet to be studied.
In the envisaged talk, we review some recent and present some new both exact and numerical results for the behavior of the Casimir and Helmholtz force. We find that all significant results are consistent with the expectations of finite size scaling theory, for which its basic postulates will be recalled.
If a material body is immersed in such a medium, its shape and the properties of its constituents modify the properties of the surrounding medium and its fluctuations. If in the same medium there is a second body then – in addition to all direct interactions between them – the modifications due to the first body influence the modifications due to the second body. This mutual influence results in a force between these bodies. If the excitations of the medium, which mediate the effective interaction between the bodies, are massless, this force is long-ranged and nowadays known as a *Casimir force*. If the fluctuating medium consists of a confined electromagnetic field in a vacuum, one speaks of the *quantum mechanical Casimir effect*. In the case that the order parameter of material fields fluctuates - such as differences of number densities or concentrations - and that the corresponding fluctuations of the order parameter are long-ranged, one speaks of the *critical Casimir effect*. This holds, e.g., in the case of systems which undergo a second-order phase transition and which are thermodynamically located near the corresponding critical point, or for systems with a broken continuous symmetry exhibiting Goldstone mode excitations. Here we review the currently available *exact results* concerning the critical Casimir effect in systems encompassing the one-dimensional Ising, XY, and Heisenberg models, the two-dimensional Ising model, the Gaussian and the spherical models, as well as the mean-field results for the Ising and the XY model. We present results both for the case of classical critical fluctuations if the system possesses a critical point at a non-zero temperature, as well as the case of quantum systems undergoing a continuous phase transition at zero temperature as a function of certain parameters. As confinements, we consider the film, the sphere-plane, and the sphere-sphere geometries. We discuss systems governed by short-ranged, by subleading long-ranged (i.e., of the van der Waals type), and by leading long-ranged interactions. In order to put the critical Casimir effect into the proper context and in order to make the review as self-contained as possible, basic facts about the theory of phase transitions, the theory of critical phenomena in classical and quantum systems, and finite-size scaling theory are recalled. Whenever possible, a discussion of the relevance of the exact results towards an understanding of available experiments is presented. The eventual applicability of the present results for certain devices is pointed out, too.
Some additional basic review on the Casimir effect can be found in [4-7].

References

[1] D.M. Dantchev, S. Dietrich, Critical Casimir effect: Exact results, Physics Reports 2023, 1005, 1-130, DOI: 10.1016/j.physrep.2022.12.004.

[2] D. Dantchev, J. Rudnick, Exact expressions for the partition function of the one-dimensional Ising model in the fixed-M ensemble, Phys. Rev. E 2022, 106, L042103.
[3] D. Dantchev, Fluctuation-induced interactions in micro-and nano-systems: Survey of some basic results, arXiv preprint 2023, arXiv:2307.09990.
[4] V.M. Mostepanenko, & N.N. Trunov, The Casimir effect and its applications, Clarendon Press, 1997, ISBN 978-0-19-853998-8.
[5] J. G. Brankov, D. M. Danchev, and N. S. Tonchev, Theory of Critical Phenomena in Finite-Size Systems, Scaling and Quantum Effects, Series in Condensed Matter Physics 2000, 9, World Scientific.
[6] K. Milton, The Casimir Effect: Physical Manifestations of Zero-Point Energy, World Scientific 2001, DOI: 10.1142/4505.
[7] K.A. Milton, The Casimir effect: recent controversies and progress, Journal of Physics A: Mathematical and General 2004, 37(38), R209, DOI: 10.1088/0305-4470/37/38/R01.

Comparative analysis of European fuel models for 2022 Razdel fire (Bulgaria)

N. Dobrinkova, V. Vassilev, N. Tsvetkova

Wildfires are exceeding problem for many European countries located in south parts of the continent. In the recent years there is an increase of wildfires in central and north zones of Europe, which led to the need of common fire fighting strategies and lessons learned to be exchanged among scientific communities in the affected countries. Such strategies and common policies were started to be developed as pilots in two European projects called "FirEURisk" and "Fire-Res". Both projects have as one of their major outcomes a list of European Fire Behaviour Fuel Models (FBFMs) which are developed with the same idea as the American FBFMs developed by Scott and Burgan in 2005. The FBFMs, along with the meteorological conditions and the digital terrain model (including slope, aspect, etc.) are needed for the so called fire behaviour modelling. The fire behaviour modelling is a special tool used by fire fighters and decision makers on the spot when wildfire is developing its propagation potential.
In our article we will compare and calibrate for possible future Bulgarian usage the two FBFM sets of fuel models published as outcomes in the two EU funded projects. The test zone selected by our team is located in south-east part of Bulgaria, covering the area of municipality of Elhovo near by the village of Razdel. The fire used for calibration purposes have been active in the period 10-14 August 2022 with final total burned area of 797 ha, where 560 ha were forest areas and 237 ha were grasslands and pastures. For our calibration work will be used FlamMap and FARSITE fire behaviour simulation tools with the same set of input parameters.

Analysis of Richardson's Extrapolation

I. Faragó

In this presentation we introduce and anlyse the Richardson extrapolation. We define its different variants (classical, repeated and multiplle exttrapolations), and investigate their consistency. We also consider the convergence and absolute stability properties of the methods. As a motivation, the DEM air pollution model is presented. The presentation will cover those areas I have worked on over the past 30 years with our friend and excellent colleague Krassimir Georgiev. This talk is a joint work with Ivan Dimov, Ágnes Havasi and Zahari Zlatev, and it is also a way to commemorate our dear friend.

A Novel Memetic Simulated Annealing Algorithm Applied on GPS Surveying Problem

S. Fidanova, K. Kapanova, K. Atanassov

Metaheuristic algorithms such as Genetic Algorithm (GA) [1], Simulated Annealing (SA) [2], Particle Swarm Optimization (PSO) [3], Differential Evolution (DE) [4], Ant Colony Optimization (ACO) [5] among others, are stochastic search algorithms inspired by natural phenomena and rules from biology, physics or ethology. The metaheuristic class of algorithms have been successfully implemented for variety of industrial and scientific problems [6-8] since they show a high efficiency of solving optimization problems with a large number of local solutions in the search space, wherein is difficult to discover a global optimum by the traditional search algorithms.

Simulated annealing is one of the most successesfull metaheuristic method for solving optimization problems. It can be applied on discrete as well as continues problems. In this work we propose a modified version of the simulated annealing algorithm, which we call memetic simulated annealing. The difference of our method from traditional simulated annealing is that we use set of neighbor solutions instead of only one neighbor, and the way of generating the neighbors. We test the proposed method on the problem for the training of multilayer neural networks, which can be utilized for the optimization of other multidimensional problems. We report on several numerical experiments, which validate our approach.

The term "memetic algorithm" is introduced by Moscato [9] in 1989. It means a synergy between population based approach and procedure for local improvement. The idea for memetic algorithm comes from hybrid genetic algorithm combined with local learning procedure to find better solutions close to the current ones. The name memetic comes from the words memes and genetic.

We call our simulated annealing algorithm memetic, because me generate set of neighbor solutions and the next current solution is chosen from this set. Using memetic variant of the algorithm gives more possibilities for improvements.

First we generate in a random way two new solution. For generating we use Mersenne Twister random number generator [10]. Let us consider solutions as points in multidimensional space.

Let us consider the three generated solutions as a vertexes of triangle. After that we generate other three solutions. The new three solutions are of the middle of the sides of the triangle. Thus the set of the neighbor solutions consists of five solutions.

References

[1] D. E. Goldberg, "Genetic Algorithms in Search, Optimization and Machine Learning", Addison Wesley Longman, London, 2006.
[2] S. Kirkpatrick, C.D. Gelatt Jr, M.P. Vecchi, Optimization by Simulated Annealing, Neurocomputing: foundations of research, MIT Press, (1988).
[3] J. Kennedy, R. Eberhart, (1995). Particle Swarm Optimization. Proceedings of IEEE International Conference on Neural Networks. IV. pp. 1942–1948, doi:10.1109/ICNN.1995.488968.
[4] Storn, R., Price, K. (1997). Differential evolution - a simple and efficient heuristic for global optimization over continuous spaces. Journal of Global Optimization. 11, pp. 341–359, doi:10.1023/A:1008202821328.
[5] Faris H, Hassonah MA, Ala' M, Mirjalili S, Aljarah I (2017) AlZoubi A multi-verse optimizer approach for feature selection and optimizing svm parameters based on a robust system architecture.
[6] M. Dorigo and T. Stützle, Ant Colony Optimization, MIT Press, 2004.
[7] Ventura S, Luna JM (2016) Pattern mining with evolutionary algorithms. Springer Publishing Company, Incorporated, 1st edition.
[8] Yang XS (2008) Nature-inspired metaheuristic algorithms. Luniver Press, USA.
[9] Moscato, P., On Evolution, Search, Optimization, Genetic Algorithms and Martial Arts: Towards Memetic Algorithms. Caltech Concurrent Computation Program, report 826, 1989.
[10] Matsumoto, M., Nishimura, T., Mersenne twister: a 623-dimensionally equidistributed uniform pseudo-random number generator, ACM Transactions on Modeling and Computer Simulation, 8(1), pp. 3-30, (1998).

Multi-Sampling Holder for Improved Scanning Sequences in Dental Micro-CT Examinations

I. Georgiev, M. Raykovska, N. Petkov

Dental micro-CT examinations have become an essential tool for researching dental anatomy [1,2] and assessing the efficacy of dental procedures [3]. However, these examinations typically involve scanning multiple samples sequentially, which can be time-consuming and inefficient. This proposal suggests using a multi-sampling holder to improve the scanning sequences in dental micro-CT examinations.
Analysis of the effectiveness of the holder is based on multi-stage studies in which each sample goes through a series of scans at different time intervals and after various manipulations. The research aims to prove that each sample from a different stage can be matched with the same one from any previous stage without manual matching before registration.
The multi-sampling holder allows multiple sample positions to be scanned in a single imaging session. It can hold up to six samples simultaneously, each in a separate bed, which can be studied individually or simultaneously. This approach significantly reduces the time required for scanning and improves overall efficiency.

The holder is made of floral foam and printed ABS plastic material and has a compact design, making it easy to handle and store. Moreover, the holder is straightforward to manufacture and allows the positioning of the samples with extreme precision in time. It can be used with most dental micro-CT scanners.
The proposed multi-sampling holder has the potential to significantly improve the quality of dental micro-CT examinations and reduce the cost of these procedures. It allows for faster and more efficient scanning.

Acknowledgments The financial support provided by the Bulgarian National Science Fund, grant KP-06-H27/6 from 08.12.2018 (I.G.) is gratefully acknowledged.

References

[1] Ahmed, H. M. A., Versiani, M. A., De-Deus, G., & Dummer, P. M. H. (2017). A new system for classifying root and root canal morphology. International endodontic journal, 50(8), 761–770. doi: 10.1111/iej.12685.
[2] Versiani, M. A., Martins, J., & Ordinola-Zapata, R. (2023). Anatomical complexities affecting root canal preparation: a narrative review. Australian dental journal, 68 Suppl 1, S5–S23. doi: 10.1111/adj.12992.
[3] Aksoy, U., Küçük, M., Versiani, M. A., & Orhan, K. (2021). Publication trends in micro-CT endodontic research: a bibliometric analysis over a 25-year period. International endodontic journal, 54(3), 343–353. doi: 10.1111/iej.13433.

Numerical Analysis and Model Calibration for COVID–19 Epidemic Spread

S. Georgiev, L. Vulkov

A mathematical deterministic compartment SEIR-type model is utilized to investigate the impact of COVID-19. This model is deemed appropriate since it accounts for the non-permanent immunity of the virus after infection. It is also realistic because it considers the nonlinear incidence rate and the delayed transmission dynamics [1]. The model poses a coefficient identification inverse problem, which involves reconstructing the transmission and recovery rates. These rates are crucial for medical professionals and policymakers to make informed decisions regarding the management and mitigation of the virus.
To further elaborate, the basic models assume that individuals move from the susceptible to the infected compartment and then to the recovered compartment, and once recovered, they have permanent immunity. However, the SIR-type model accounts for the fact that COVID-19 may not confer permanent immunity after recovery, making it a more appropriate model for this virus.
The identification of the transmission and recovery rates is a challenging problem that requires the use of mathematical tools such as inverse problems [2]. This process involves estimating the unknown parameters of a model from observed data, in this case, the number

of confirmed cases and recoveries. Accurately identifying these rates is essential for policymakers to make informed decisions on implementing measures to slow the spread of the virus and to allocate resources such as hospital beds and medical supplies. It also aids in the development and evaluation of effective treatments and vaccines.
The task of solving the inverse problem in this study is transformed into a minimization problem, which is tackled by finding the solution that yields the smallest squared error [3]. Once the values of the parameters are obtained, it is conducted an identifiability analysis to ensure that the estimated values are reasonable and reliable [4]. To validate the findings of the study, the results are compared with those of previous studies, using real data collected from Bulgaria. The comparison involves evaluating the consistency and accuracy of the estimated parameter values, as well as assessing the model's ability to predict the behavior of the COVID-19 epidemics.

Acknowledgments The authors are supported by the Bulgarian National Science Fund under Project KP-06-N 62/3 "Numerical methods for inverse problems in evolutionary differential equations with applications to mathematical finance, heat-mass transfer, honeybee population and environmental pollution" from 2022.

References

[1] A. Kumar, K. Goel, R. Nilam, A deterministic time-delayed SIR epidemic model: mathematical modeling and analysis, *Theory in Biosciences*, 139:67-76, 2020.
[2] Tch.T. Marinov, R.S. Marinova, COVID–19 analysis using inverse problem for coefficient identification in SIR epidemic models, *Chaos, Solitons & Fractals: X*, 100041, 2020.
[3] S.G. Georgiev, L.G. Vulkov, Coefficient identification in a SIS fractional-order modelling of economic losses in the propagation of COVID–19, *Journal of Computational Science*, 69:102007, 2023.
[4] C. Lee, Y. Li, J. Kim, The susceptible-unidentified infected-confirmed (SUC) epidemic model for estimating unidentified infected population for COVID-19, *Chaos, Solitons & Fractals*, 139:110090, 2020.

Numerical Solution of a Free Boundary Problem for a Saturated-Unsaturated Water Flow Absorption in Soil

T. Gyulov, J. Kandilarov

A free boundary value problem from hydrology considered in [1-3] is studied numerically. It is a nonlinear model which represents the development of zones of saturation in wetted soils which appear naturally in the vicinity of surface ponds, subterranean cavities and other

bodies of water. The problem has the following form

$$\frac{\partial\theta}{\partial t} = \frac{\partial}{\partial x}\left[D(\theta)\frac{\partial\theta}{\partial x}\right], \quad x > s(t), t > 0 \tag{1}$$

$$\theta(s(t)^+, t) = \theta_s, t > 0 \tag{2}$$

$$-D(\theta)\frac{\partial\theta}{\partial x}(s(t)^+, t) = K_s\frac{\Psi_0 - \Psi_s}{s(t)}, \quad t > 0, \tag{3}$$

$$\theta(x, 0) = \theta(+\infty, t) = \theta_n = \text{const}, \text{x} > 0, \text{t} > 0 \tag{4}$$

Here θ is the volumetric water content, $s(t)$ is the free boundary which separates the saturated zone (the interval $[0, s(t)]$ in the variable x) from the unsaturated zone $x > s(t)$ at time t, Ψ_0 and Ψ are the pressure head at $x = 0$ and the soil water matric potential, respectively, K is the hydraulic conductivity and $D = K\frac{\mathrm{d}\Psi}{\mathrm{d}\theta}$ is the soil water diffusivity. The subindex s denotes the values of the corresponding quantities at saturation.
If Kirchoff's transformation is applied

$$u(\theta) := K_s\Psi_s + \int_{\theta_s}^{\theta} D(\eta)\mathrm{d}\eta, \tag{5}$$

for $\theta \leq \theta_s$, then problem (1)-(3) is equivalent to

$$\frac{\partial\theta}{\partial t} = \frac{\partial^2 u}{\partial x^2}, \quad x > 0, t > 0 \tag{6}$$

$$u(0, t) = K(\Psi_0)\Psi_0, \quad t > 0 \tag{7}$$

$$u(x, 0) = u(+\infty, t) = u_n := u(\theta_n), x > 0, t > 0 \tag{8}$$

where

$$\theta(y) := \begin{cases} u^{-1}(y) & \text{if} \quad y < u_s \\ \theta_s & \text{if} \quad y \geq u_s \end{cases}$$

and u^{-1} is the inverse of $u(\theta)$ defined in (5). Note that the solution of (6)-(8) satisfies $u \equiv K\Psi$. In addition, it is singular at $x = 0$, $t = 0$ since the initial condition (8) is incompatible with the left boundary condition (7), $K(\Psi_0)\Psi_0 \neq u_n$.
More generally, we consider equation (6) with an additional source term f. In order to deal with the difficulty caused by the singularity of the solution we propose a suitable transformation of the space and time variables. We apply numerical scheme of Crank - Nicolson type combined with immersed interface method and obtain numerical solution of second order of convergence in space and time.

Acknowledgements This research is supported by the Bulgarian National Science Fund under the Project KP-06-N 62/3 "Numerical methods for inverse problems in evolutionary differential equations with applications to mathematical finance, heat-mass transfer, honeybee population and environmental pollution", 2022.

References
[1] Briozzo A.C., Tarzia D.A.: Explicit solution of a free boundary problem for a nonlinear absorption model of mixed saturated–unsaturated flow. Adv. Water Resour., **21**(8), 713–721 (1998).
[2] Broadbridge P.: Solution of a nonlinear absorption model of mixed saturated-unsaturated flow. Water Resour. Res. **26**(10), 2435–2443 (1990).
[3] Broadbridge P., White I.: Constant rate rainfall infiltration: a versatile nonlinear model 1. Analytic solution. Water Resour. Res. **24**(1), 145–154 (1988).

Mathematical Modeling of the Epidemic Dynamics of COVID-19 in Bulgaria by SEIRS Model with Vaccianation

T. Hristov

This talk is based on joint work with Svetozar Margenov, Nedyu Popivanov, Iva Ugrinova, Stanislav Harizanov in progress or already published in [1–4].
Since the end of 2019, with the outbreak of the new coronavirus disease COVID-19, the world has changed entirely in many aspects. The pandemic has affected economies, healthcare systems and global society. Unfortunately, Bulgaria has the second-highest COVID - 19 mortality rate in the world and the lowest vaccination rate in the European Union. To understand the reason for this situation and to analyze the long-term SARS-CoV-2 outbreak dynamics we introduce an extended time-dependent SEIRS model SEIRS-VB with vaccination and vital dynamics. We carry out a mathematical analysis to illustrate some biological reasonable properties of the differential model SEIRS-VB, such as the non-negativity, boundedness, existence, and uniqueness. To apply the model SEIRS-VB we develop some numerical simulation tools and for this reason we introduce a family of time-discrete variants. Further, we solve suitable inverse problems for the identification of parameters in discrete models and propose a methodology for selecting a discrete model from the constructed family, which has the closest parameter values to these in the differential model SEIRS-VB. This allows us to find the behavior over time of some crucial epidemiological parameters, such as the transmission rate, the recovery rate, and the basic reproduction number. To validate the studied models, we use Bulgarian COVID-19 data. Based on the presented analysis, we develop a strategy for short-term prediction of the spread of the virus among the host population.

References
[1] Margenov, S.; Popivanov, N.; Ugrinova, I.; Hristov, Ts. Differential and Time–Discrete SEIRS Models with Vaccination: Local Stability, Validation and Sensitivity Analysis Using Bulgarian COVID-19 Data. *Mathematics* **2023**, *11(10)*, 2238, https://doi.org/10.3390/math11102238.
[2] Margenov, S.; Popivanov, N.; Ugrinova, I.; Hristov, Ts. Mathematical Modeling and Short-Term Forecasting of the COVID-19 Epidemic in Bulgaria: SEIRS Model with Vaccination. *Mathematics* **2022**, *10(15)*, 2570, https://doi.org/10.3390/math10152570.
[3] Margenov, S.; Popivanov, N.; Ugrinova, I.; Harizanov, S.; Hristov, Ts. Parameters Identification and Forecasting of COVID-19 Transmission Dynamics in Bulgaria with Mass Vaccination Strategy. *AIP Conf. Proc.* **2022**, *2505*, 080010, https://doi.org/10.1063/5.0106519.

[4] Margenov, S.; Popivanov, N.; Ugrinova, I.; Harizanov, S.; Hristov, Ts. Mathematical and Computer Modeling of COVID-19 Transmission Dynamics in Bulgaria by Time-depended Inverse SEIR Model. *AIP Conf. Proc.* **2021**, *2333*, 090024, https://doi.org/10.1063/5.0041868.

Perspectives from large-scale *in silico* studies of multicomponent solutions of putative antimicrobial peptides

N. Ilieva, E. Lilkova, P. Petkov, L. Litov

Antimicrobial peptides (AMPs) have attracted significant scientific interest over the past few decades due to their role as the host's primary defense against microbial invasion. Building on previous research we present an *in silico* perspective of a new concept of the mechanism of action of antimicrobial peptides, with an emphasis on the possible modes of action and biological role of non-cationic peptides on the example of newly isolated peptides from the fraction of the mucus of the garden snail *C. aspersum* below 3 kDa. Based on large-scale molecular dynamics and metadynamics simulations, we argue that linear AMPs self-associate in the body fluids in nanoscale aggregates in a balance between electrostatic and hydrophobic interactions. These aggregates (clusters) represent the perfect transport system: locking the hydrophobic uncharged residues in the core of the cluster prevents the interaction with the eukaryotic membranes with lower surface charge density, and positioning the charged residues on the cluster surface enables for electrostatic interaction with the bacterial surface. Furthermore, the peptide folding promoted by the amphiphilic structure in the aggregate allows a sufficiently high local concentration of AMPs to be delivered to the target membrane in a functionally active conformation. Our studies also show that the effect of AMP charge on the energetics of the peptide-membrane interaction is not as straightforward as assumed *a priori*. While the positive charge is required to electrostatically conduct the AMP to the target membrane, the presence of neutral hydrophobic domains in the AMP molecule is necessary to drive membrane embedding via the hydrophobic effect, and a negatively charged domain can be beneficial to enhance membrane penetration and pore formation.

Acknowledgments This work is partially supported by the Bulgarian Science Fund (Grant KP-06-OPR 03-10/2018).
Computational resources were provided by CI TASK (Centre of Informatics–Tricity Academic Supercomputer & networK), Gdansk (Poland), as well as the BioSim HPC cluster at the Faculty of Physics, Sofia University "St. Kliment Ohridski".

Construction and Realization of Nonstandard Difference Schemes for SIR and SEIR Models with and without Spatial Diffusion

M. Koleva, L. Vulkov

In recent years many authors using the compartmental models theory have studied the spreading of COVID-19 in countries of interest. One typical model that describes this kind of population is the following semilinear parabolic initial boundary-value problem in the region $Q_T = \{(t,x) : t \in (0,T),\ \ x \in \Omega \subset R^2\}$

$$\frac{\partial S}{\partial t} = d_S \triangle S + \Lambda - (\beta I + \mu) S, \tag{9}$$

$$\frac{\partial E}{\partial t} = d_E \triangle E + \beta S I - (\mu + \gamma) E, \tag{10}$$

$$\frac{\partial I}{\partial t} = d_I \triangle I + \gamma E - (\mu + \alpha) I, \tag{11}$$

$$\frac{\partial R}{\partial t} = d_R \triangle R + \alpha I - \mu R, \tag{12}$$

$$S(0,x) = S_0(x),\ \ E(0,x) = E_0(x),\ \ I(0,x) = I_0(x),\ \ R(0,x) \in R_0(x),\ \ x \in \Omega,$$

$$\frac{\partial S(t,x)}{\partial n} = \frac{\partial E(t,x)}{\partial n} = \frac{\partial I(t,x)}{\partial n} = \frac{\partial R(t,x)}{\partial n} = 0 \ \text{ for } \ x \in \partial\Omega,\ \ t \in (0,T),$$

$$\int_\Omega \left(S(0,x) + E(0,x) + I(0,x) + R(0,x)\right) dx = N_0 = \text{ constant.}$$

Here $S(t,x)$ denotes the susceptible population, $E(t,x)$ is the exposed population to COVID-19 by the contact with an infected, $I(t,x)$ denotes the infected population, $R(t,x)$ is the population of removed/recovered; $\beta > 0$ is the transmission rate from the susceptible population to the infected population, $\Lambda > 0$ compares the births and new residents per unit value of time, $\mu > 0$ is the rate of death, $\gamma > 0$ is the transmission rate of confirmed infected people from the exposed population ($1/\gamma$ is the duration of the latent period).) $\alpha > 0$ is the remove/recovery rate from the infected population (the time spent in the "infectious" compartment is $1/\alpha$, $d \equiv (d_S, d_E, d_I, d_R)$ denotes the diffusion coefficient of the population $S(t,x)$, $E(t,x)$, $I(t,x)$ and $R(t,x)$, respectively.
In the particular case of system (9)-(12) when formally we take $\mu = \gamma = 0,\ E \equiv 0$ and instead of equation (11) we use

$$\frac{\partial I}{\partial t} = d_I \triangle I + \beta S I - \alpha I. \tag{13}$$

The resulting system is referred as SIR model.

The system (9)-(12) is written in *productive-destructive* form [1,2]. Letting

$$N(t) = \int_{\Omega} (S(t,x) + E(t,x) + I(t,x) + R(t,x))dx, \quad N(0) = N_0,$$

one can derive the inequality

$$\frac{dN}{dt} \leq \Lambda|\Omega| - \mu N(t),$$

called generalized conservation law (CL) [1,2].
For the corresponding SIR ordinary differential equation (ODE) model of (9), (11), (12)

$$\begin{aligned} \frac{\partial S}{\partial t} &= \Lambda - (\beta I + \mu)S, \\ \frac{\partial I}{\partial t} &= \beta SI - \alpha I, \\ \frac{\partial R}{\partial t} &= \alpha I - \mu R, \end{aligned} \tag{14}$$

the global dynamics is determined by the basic reproduction.

The goals of the present work are:

(i) Derivation of positive dynamically consistent nonstandard difference scheme [1,2] for the ODEs (14) and for (9)-(12) or (9), (13) and (11) after standard approximation of the Laplacian $\triangle$, satisfying the conservation law.

(ii) Development of simpler than Newton's method iterations, namely Jacobi and Gauss-Seidel iterations for realization of implicit difference schemes equations of the SEIR and SIR models.

(iii) Computational experiments compare the merits of (ii) iterative methods and Anderson a fixed points acceleration.

References

[1] R.E. Mickens, Nonstandard Finite Difference Schemes: Methodology and Applications, World Scientific, 2020.

[2] D.T. Wood, D.T. Dimitrov, H.V. Kojouharov, A nonstandard finite difference method for n-dimensional productive destructive systems, Journal of Difference Equations and Applications 21, 2015, 240–254.

Simultaneous Identification of Two Coefficients in Reaction Diffusion Systems from Final- time Measurements

M. Koleva, L. Vulkov

In this work we study a class of parabolic inverse problems where unknown coefficients of reaction diffusion system are space-dependent and extra conditions are final-time measure-

ments. More precisely, let Ω be a bounded domain in R^2 with piecewise smooth boundary $\partial\Omega$ and $Q_T = \Omega \times (0,T]$ with $T > 0$. We will find the quadruplet of functions $(u(x,y,t), v(x,y,t)), (a(x,y), d(x,y))$ which solve the following problems:

$$\frac{\partial u}{\partial t} = d\triangle u + a(x,y)u + b(x,y)v = 0, \quad (x,y,t) \in Q_T, \tag{15}$$

$$\frac{\partial v}{\partial t} = d\triangle v + c(x,y)u + d(x,y)v = 0, \quad (x,y,t) \in Q_T, \tag{16}$$

with Dirichlet boundary conditions

$$u|_{\partial\Omega} = f(x,y,t), \quad v|_{\partial\Omega} = g(x,y,t), \quad (x,y) \in \partial\Omega, \quad 0 < t \leq T, \tag{17}$$

initial conditions

$$u(x,y,0) = u_0(x,y), \quad v(x,y,0) = v_0(x,y), \quad (x,y) \in \partial\Omega \tag{18}$$

and two extra measurements

$$u(x,y,T) = \varphi(x,y), \quad v(x,y,T) = \Psi(x,y), \quad (x,y) \in \Omega. \tag{19}$$

In the particular case when

$$a(x,y) = c(x,y) = \mu(x,y), \quad b(x,y) = -d(x,y) = -\alpha(x,y)$$

the problem above describes honeybee collapse due to pesticide contamination, see e.g. [1]. We use the overspecified information (19) to transform the inverse coefficient problem (15)-(19) to forward problem with nonlocal terms in the differential equations and the initial conditions. For numerical solution of the last problem, we first apply semidiscreteization in space. Then, the resulting non-linear system of ordinary differential equations (ODEs) is discretized by three iterative numerical scheme, using different time steppings.
Numerical simulations using synthetic and real measured data are discussed.

References

[1] P. Magal, G.F.Webb, A spatial model of honeybee colony collapse due to pesticide contamination of forager bees, J. Math. Biol., 2020, 80, 2363–2393

Machine Learning and Computer Vision for Collecting of Statistical Data from Vegetable Fields

V. Kotev, I. Ivanov, S. Ranchev, M. Ivanova, P. Dobreva

In the resent years' machine learning has being applied to various arias of agriculture. Machine learning (ML) plays a crucial role in addressing weed-related issues in agriculture. ML algorithms, particularly those based on deep learning, can learn intricate patterns and

features, making them well-suited for the nuanced task of weed detection. In the present research deep learning algorithms such as YOLOv5 and SORT are applied to detect and to track vegetables and weeds based on computer vision. Moreover, an object tracker SORT is utilizing and adjust to assign to each vegetable and weed unique number. First, datasets of annotated images of cabbage and weed are created. Then, the ML algorithm YOLOv5 for object detection is selected. Next, YOLOv5 is trained to detect cabbage and weed form our annotated datasets. The accuracy of the model performance is studied. Finally, he created object detector and tracker provide significant information about the distribution and sizes of weed vegetables in the given areas. This lead to efficient weed treatment procedure.

Introduction Weeds pose a significant threat to agriculture, causing substantial damage to crop yields and diminishing the overall quality of agricultural production. The annual impact of weed infestation surpasses losses incurred from diseases and pests combined. Effective weed management stands as a pivotal element in agricultural practices. Globally, there is a trend towards reducing the relative workforce in agriculture through the integration of comprehensive mechanization and chemical solutions. To achieve significant biological and economic benefits from weed control, a thorough understanding of their modes of propagation, as well as their morphological, biological, and ecological characteristics, is imperative. Weeds exert harmful effects on cultivated plants, impacting production efficiency both directly and indirectly. ML models, once trained on diverse datasets, can provide efficient and precise identification of weeds in real-time. This enables timely interventions, such as targeted herbicide application or mechanical removal, minimizing the impact on crops while effectively managing weed populations. Agriculture often involves vast expanses of land, making manual weed detection and management labor-intensive and time-consuming. ML allows for the scalability of weed detection processes, enabling the analysis of large agricultural areas efficiently and accurately.
The aim of the research is to develop based on computer vision and existing machine learning algorithms object detection and tracking system for vegetables and weeds.

Development of object detection and tracking system for cabbage and weed Creating an object detection system involves several steps. The first we collected and Labeled Data. A video moves of the field with cabbage is shot. Then video is split into frames. After, that cabbage and weed are labeled. Bounding boxes indicating locations of the cabbage and weed as well as their sizes. Then our dataset is divided into training, validation, and test sets. Deep Learning classification framework supports object detection. Next, a Pre-trained Model is studied and selected. Models like YOLO (You Only Look Once), SSD (Single Shot Multibox Detector), and Faster R-CNN (Region-based Convolutional Neural Network) are commonly used for object detection tasks. YOLOv5 model is selected for our research. Then, we adapt and adjust this model to our datasets of cabbage and weeds. This process allows the model to learn the specific characteristics of the cabbage and weed (objects) to detect. The model using our annotated dataset is trained. This involves adjusting the model's weights based on the differences between its predictions and the ground truth labels. Training may take some time, depending on the complexity of the model and the size of dataset. Assess the model's performance on the validation set to ensure it generalizes well to new

data. The SORT algorithm for object tracking is adjusted to our dataset to assign ID to the target cabbage and weeds. The object tracker could count each cabbage and weed with low error.

Conclusion A SORT object tracking algorithm is adapted to track and assign ID to each cabbage and weeds on videos. Moreover, the tracker will provide the information about the quantities of the cabbage and weed in the treated area. The dimensions of each cabbage and weed could be measured from the bounding boxes of the object detector.

Acknowledgments This work was supported / (partially supported) by the Bulgarian Ministry of Education and Science under the National Research Programme „Smart crop production“ approved by Decision of the Ministry Council No 866 / 26.11.2020.

References

[1] Redmon, S. Divvala, R. Girshick and A. Farhadi,"You Only Look Once: Unified, Real-Time Object Detection," 2016 IEEE Conference on Computer Vision and Pattern Recognition (CVPR), Las Vegas, NV, USA, 2016, pp. 779-788

[2] Bewley, Z. Ge, L. Ott, F. Ramos and B. Upcroft,"Simple online and realtime tracking" 2016 IEEE International Conference on Image Processing (ICIP), Phoenix, AZ, USA, 2016, pp. 3464-3468, doi: 10.1109/ICIP.2016.7533003.

Inhibiting the SARS-CoV-2 protein ORF6: a computational study

E. Lilkova, P. Petkov, M. Rangelov, N. Todorova, N. Ilieva, and L. Litov

Although COVID-19 greatly reduced in mortality rates, the desease still poses a serios public health challenge due to various long-lasting negative health effects. The pathogenicity of the SARS-CoV-2 virus is associated with the action of one of its accessory proteins – the Open Reading Frame 6 (ORF6), the most toxic protein of the virus. This small protein plays a crucial role in immune evasion by antagonizing the host cell interferon signaling pathways, thus limiting the immune response to the infection. Blocking its activity is however greatly held up by the lack of experimentally resolved 3D structure of this protein.

Here we report our *in silico* investigaion of the structure and mechanism of action of the SARS-CoV-2 ORF6 protein. A 3D structural model of the protein, embedded in a model endoplasmic reticulum membrane was developed using molecular modelling. We demonstrate that ORF6 accomplishes its effects by binding the ribonucleic acid export 1 (RAE1) protein and sequestering it in the cytoplasm. RAE1 binds to multiple ORF6 molecules simultaneously and very stably, which anchors it to the ER membranes in the cytoplasm. These observations were confirmed experimentally by studying the co-localisation of both proteins in ORF6 overexpressing and control cells.

Acknowledgments This research was partially funded by the Bulgarian National Science Fund under Grant KP-06-DK1/5/2021 SARSIMM.
Computational resources were provided by CI TASK (Centre of Informatics–Tricity Academic Supercomputer & networK), Gdansk (Poland), as well as the BioSim HPC cluster at the Faculty of Physics, Sofia University "St. Kliment Ohridski".

Strang splitting for fractional-in-space diffusion-reaction equations

S. Margenov

We consider the time-dependent system

$$\begin{aligned} \frac{du_k(x,t)}{dt} &= \mathcal{L}_k^{\alpha_k} u_k(x,t) + \mathcal{R}_k(u_1,\ldots,u_m) + f_k(x,t), \quad k=1,\ldots,m, \\ u_k(x,t) &= 0, \quad x \in \partial\Omega, \\ u_k(x,0) &= u_{k,0}(x), \end{aligned} \tag{20}$$

where $u_k(x,t)$ are unknown, $x \in \Omega \subset \mathbb{R}^d$, $d \in \{2,3\}$, $t \in [0,T]$, $0 < \alpha_k < 1$. The elliptic operators $\mathcal{L}_k$ correspond to the bilinear forms

$$(v,w)_{\mathcal{L}_k} = \int_\Omega a_k(x) \nabla v(x) \cdot \nabla w(x) dx, \quad 0 < \underline{a}_k \le a_i(x).$$

The spectral definition of $\mathcal{L}^\alpha$ applies, i.e.

$$\mathcal{L}^\alpha v(x) = \sum_{i=1}^{\infty} \lambda_i^\alpha c_i \phi_i(x), \;\; \mathcal{L}^{-\alpha} v(x) = \sum_{i=1}^{\infty} \lambda_i^{-\alpha} c_i \phi_i(x), \;\; c_i = \int_\Omega v(x)\phi_i(x)dx,$$

where $0 < \alpha < 1$, $\{\phi_i(x)\}_{i=1}^\infty$ are the orthonormal eigenfunctions of $\mathcal{L}$, and $0 < \lambda_1 \le \lambda_2 \le \ldots$ are the related eigenvalues. Following [1,2] we write (20) in the abstract Cauchy form

$$\begin{aligned} \frac{d\mathbf{u}}{dt} &= (\mathcal{A}+\mathcal{B})\mathbf{u}, \quad t \in [0,T] \\ \mathbf{u}(0) &= \mathbf{u}_0, \end{aligned} \tag{21}$$

where $\mathcal{A}$ and $\mathcal{B}$ correspond to the fractional diffusion and the reaction plus source parts of (20) respectively, and $\mathbf{u} = (u_1,\ldots,u_m)^T$, $\mathbf{u}_0 = (u_{1,0},\ldots,u_{m,0})^T$. The operator $\mathcal{A}$ is non-local and decoupled with respect to the unknowns u_k while $\mathcal{B}$ couples the system but is fully local in space.

STRANG SPLITTING ALGORITHM

Step 1:

$$\begin{aligned} \frac{d\mathbf{u}_1^j}{dt}(t) &= \mathcal{A}\mathbf{u}_1^j(t), & (j-1)\tau < t \le (j-0.5)\tau, \\ \mathbf{u}_1^j((j-1)\tau) &= \mathbf{u}_3^{j-1}((j-1)\tau), \end{aligned}$$

Step 2:

$$\begin{aligned} \frac{d\mathbf{u}_2^j}{dt}(t) &= \mathcal{B}\mathbf{u}_2^j(t), & (j-1)\tau < t \le j\tau, \\ \mathbf{u}_2^j((j-1)\tau) &= \mathbf{u}_1^j((j-0.5)\tau), \end{aligned}$$

Step 3:

$$\begin{aligned} \frac{d\mathbf{u}_3^j}{dt}(t) &= \mathcal{A}\mathbf{u}_3^j(t), & (j-0.5)\tau < t \le j\tau, \\ \mathbf{u}_3^j((j-0.5)\tau) &= \mathbf{u}_2^j(j\tau), \end{aligned}$$

$j = 1, 2, \ldots, J$, $\tau = T/J$ is the time step.
The Crank-Nicolson method is applied in Step 1 and Step 2, which is combined in Step 2 with a Runge-Kutta scheme of appropriate order to ensure second-order accuracy with respect to τ. Finite differences or linear finite elements are used for discretization in space providing accuracy of order $O(h^{2\alpha_k})$. Here, $h = O(N^{-d})$ is the mesh parameter corresponding to N degrees of freedom in space. A key issue of the proposed algorithm concerns Step 1 and Step 3, where the non-local fractional diffusion operator $\mathcal{A}$ is included. The study is a further development of [1] where the efficient implementation of the sequential splitting algorithm is discussed.
A new challenge is that Step 1 and Step 3 involve both, numerical solution of non-local linear systems with dense matrices $L_k^{\alpha_k} + qI$ and matrix vector multiplications with $L_k^{\alpha_k}$. The symmetric and positive definite sparse matrices L_k correspond to the diffusion operators $\mathcal{L}_k$, $q = 1/\tau$. Here we use methods based on best uniform rational approximation (BURA) of $\xi^\alpha/(1 + q\xi^\alpha)$ and $\xi^{1-\alpha}$ for $\xi \in [0, 1]$ and $\alpha \in (0, 1)$.
An important feature of the BURA methods is that non-local linear algebra problems reduce to a number of local systems with matrices such as $L_k + t_k I$, $t_k > 0$. We assume that fast iterative solver is used for these systems. It may surprise some readers that in Step 1 and Step 3 matrix vector multiplications are computationally more difficult than solving the corresponding linear systems. The proposed method has nearly optimal computational complexity of order $O(JN \log N)$. Errors of different origin are balanced in a way that ensures accuracy of order $O(h^{2\alpha} + \tau^2)$, $\alpha = \min_k \alpha_k$.

Acknowledgements The partial support through the Bulgarian NSF Grant KP-06 PN7215 is acknowledged.

References
[1] K. Georgiev, S. Margenov, Numerical Methods for Fractional Diffusion-Reaction Problems Based on Operator Splitting and BURA, Advanced Computing in Industrial Mathematics, Studies in Computational Intelligence, Springer, Cham., Vol. 1111 (2023), 73-84
[2] I. Farago, Splitting Methods and Their Application to the Abstract Cauchy Problems, Springer LNCS, Vol. 3401 (2005), 35-45
[3] S. Harizanov, R. Lazarov., S. Margenov, P. Marinov, J. Pasciak, Analysis of numerical methods for spectral fractional elliptic equations based on the best uniform rational approximation, Journal of Computational Physics, Vol. 408 (2020), https://doi.org/10.1016/j.jcp.2020.109285

IoT Cybersecurity Certification – A Multicriteria Assessment Approach

R. Menda-Shabat-More, Z. Minchev

Modern digital Web 3.0 reality is presently dependent on IoTs & AI technologies' diverse development, addressing new smart solutions for peoples living, working & even entertaining [1]. Properly understanding the cybersecurity asset in this transformational process is of vital importance for successful achievement of multiplatform certification and thus industrial standardization with this innovative productional area [2]. The study presents a modelling approach for an initial identification of cybersecurity assets, following a set of expert criteria joint extended fuzzy evaluation [3]. Further, the obtained results are validated with stochastic simulations and finally compared with real-life industrial experiments. The presented approach gives a flexible solution to the IoT cybersecurity certification problem, joining both machine and human intelligence towards an industrial standartisation of the process with real products' working experience.

References
[1] Minchev, Z. et al. Digital Transformation in the Post-Information Age, Institute of ICT, Bulgarian Academy of Sciences & Softtrade, 2022
[2] Menda-Shabat-More, R., Minchev, Z. Private Schemes for Cybersecurity Certifications: An Experimental Modeling and Forecasting for Success, In Proc. of BISEC 2023, Belgrade Metropolitan University, Nis, Serbia, Nov 24, 2023 (in press)
[3] Minchev, Z. Human Factor Dual Role in Modern Cyberspace Social Engineering, NATO Science for Peace and Security Series - D: Information and Communication Security, Volume 42: Terrorist Use of Cyberspace and Cyber Terrorism: New Challenges and Responses, 2015, pp. 116 – 128, DOI: 10.3233/978-1-61499-528-9-116 nline and realtime tracking" 2016 IEEE International Conference on Image Processing (ICIP), Phoenix, AZ, USA, 2016, pp. 3464-3468, doi: 10.1109/ICIP.2016.7533003.

The Convection-Diffusion Problem: Remembrance of Working With Krassimir Georgiev

M. Neytcheva

In this presentation we consider the very classical stationary convection-diffusion equation

$$\mathcal{L}_\varepsilon\, u \equiv -\varepsilon \Delta u \,+\, \boldsymbol{v}\cdot\nabla u \quad = f(\boldsymbol{x}),\, \boldsymbol{x}\,\in\,\Omega,$$

where $\Omega \in \mathbf{R}^d$ is a bounded domain with a boundary $\partial\Omega$, $d = 1, 2, 3$, $\varepsilon > 0$ and $\boldsymbol{v}(\boldsymbol{x})$ is the velocity field.

Suitable discretization methods and numerical solution methods for the convection-diffusion problem have been considered since many years and there exist deep understanding on how to approach the numerical solution of this problem.

The continuous problem carries several characteristics, which must be properly incorporated in the discretization method in order to ensure that the discrete solution is accurate enough and preserves the properties of the continuous problem. The choice of a discretization method, in turn, influences the choice and the performance of the numerical solution method to solve the arising algebraic systems of equations.

It is well known that numerical difficulties with this equation are encountered when we deal with convection-dominated convection-diffusion problems, referred also to as singularly perturbed, namely, when ε is small. When $\varepsilon \to 0$, the convection term dominates. The solutions of problems of the considered type are characterized by different kinds of layers which depend on the boundary conditions as well as on the velocity field $\boldsymbol{v}$. Also, for ensuring stability of the discretization, in many cases the matrix in the resulting algebraic linear system is non-symmetric.

In this presentation we consider some insightful cases to enlighten these difficulties and how to possibly approach them. We assume that the flow is potential, i.e., in three dimensions its velocity field $\boldsymbol{v}(\boldsymbol{x}) = [v_1(\boldsymbol{x}), v_2(\boldsymbol{x}), v_3(\boldsymbol{x})]^T$ is a gradient of a velocity potential ϕ, such that

$$\boldsymbol{v} = \nabla\phi.$$

The benefit of having a potential vector field is that we can apply a certain exponential transformation and symmetrize the differential operator. Multiplying both sides in the convection-diffusion equation by $\varepsilon^{-1}e^{-\frac{\phi}{\varepsilon}}$ we transform the differential operator $\mathcal{L}_\varepsilon$ to a selfadjoint one:

$$\widetilde{\mathcal{L}}_\varepsilon \;=\; -\left[\frac{\partial}{\partial x_1}\left(e^{-\frac{\phi}{\varepsilon}}\frac{\partial u}{\partial x_1}\right) + \frac{\partial}{\partial x_2}\left(e^{-\frac{\phi}{\varepsilon}}\frac{\partial u}{\partial x_2}\right) + \frac{\partial}{\partial x_3}\left(e^{-\frac{\phi}{\varepsilon}}\frac{\partial u}{\partial x_3}\right)\right] \;=\; \varepsilon^{-1}\, e^{-\frac{\phi}{\varepsilon}}\, f(\boldsymbol{x}).$$

Such a transformation is called an *exponential fitting*.

The linear system resulting from discretizing the operator $\widetilde{\mathcal{L}}_\varepsilon$ becomes then symmetric and positive definite, and can be solved with the conjugate gradient method, preconditioned with some well-developed optimal preconditioning technique, such as the Algebraic Multigrid (AMG) method or the Algebraic Multilevel Iteration (AMLI) method. We discuss the advantages and the disadvantages of the approach and illustrate those with some numerical tests.

The above study was done together with Prof. Krassimir Georgiev in [1,2]. This presentation is a remembrance of the collaborative work done together with him as well as the long-term friendship, maintained through more than 35 years.

References

[1] M. Neytcheva, O. Axelsson and K. Georgiev, An application of the AMLI method for solving convection-diffusion problems with potential velocity field. In O. Axelsson and B. Polman (eds.), *Proceedings of the conference on Algebraic Multilevel Iteration Methods with Applications*, Nijmegen, June 13-15, 1996, 197–210.

[2] O.Axelsson, K.Georgiev, M.Neytcheva, Symmetric numerical scheme for some convection-diffusion problems. In S. Markov (ed.), *Proceedings of the International Conference on Mathematical Modelling and Scientific Computation*, Sozopol, Bulgaria, September 14-18, 1993. Datecs Publishing, Sofia, 55–58.

Several solitary wave solutions of conformable time-fractional Wu–Zhang system via Simple Equations Method (SEsM)

E. Nikolova

In this study we focus on consideration of the nonlinear Wu-Zhang system with fractional derivative order. The system represents the propagation of dispersive long waves on shallow waters. By introducing conformable fractional transformation the nonlinear fractional partial differential equations are reduced to nonlinear ordinary differential equations with integer order. We apply the Simple Equations Method (SEsM) for obtaining exact analytical solutions of the reduced system. The solution of the system equations is constructed as a composite function of two functions of two independent variables. The two composing functions are finite series of the solutions of two simple equations.The simple equations used for this study are ordinary differential equations (ODEs) of first order, such as the ODE of Riccati, the ODE of Bernouli and the ODE of Abel of first kind. Numerical simulations of several analytical solutions are made to demonstrate the possible solitary waves which can appear in the considered medium.

Deploying data-driven models for turbulence closure modeling in computational fluid dynamics numerical solvers

P. Petkov, V. Pavlov, L. Nista, T. Grenga, H. Pitsch, S. Markov

In recent decades, the remarkable capabilities demonstrated by deep learning frameworks in capturing intricate nonlinear interactions have opened new modeling strategies for advancing beyond conventional physics-based models. Among the different approaches and

techniques currently available, the super-resolution (SR) approach, which generates high-resolution fields from low-resolution fields, is a promising approach for turbulence closure. Several works available in the literature have evaluated its performance in a priori fashion, where the modeled subgrid-scales (SGS) terms occurring in the large-eddy simulation (LES) were compared with the exact solution computed from direct numerical simulations (DNS), often achieving outstanding performance and outperforming standard equation-based model. Despite such encouraging conclusions, model configurations must also demonstrate their validity in an a posteriori manner, in which the data-driven SGS model is coupled to an LES numerical solvers. The applicability of those models hinges not only on the specific training approach employed but also on their seamless integration into computational fluid dynamics (CFD) codes. Thus, it is fundamental to understand how to embed data-driven models into LES solvers optimally, as this integration facilitates a more comprehensive analysis, faster execution time, and better predictive and robustness capabilities — a process of paramount significance for high-performance LES.

In this work, we present an innovative approach for integrating data-driven models into CFD codes, facilitating the seamless incorporation of advanced simulation techniques into the realm of Large Eddy Simulation. The SuperLES library, following the separation of concerns principle in software engineering, encapsulates the ML algorithm. It is designed to be highly configurable and model-agnostic, ensuring smooth integration with different ML architectures. The library's compatibility with the open neural network exchange (ONNX) format facilitates easy storage and retrieval of raw machine learning (ML) models, aligning with ONNX runtime for efficient execution across various frameworks, operating systems, and hardware platforms. To address the computational demands of large-scale simulations, a domain decomposition approach is implemented to break down the velocity field into subregions. This approach enables parallel computing, effectively utilizing available resources for accelerated solutions. Additionally, subdomain decomposition is introduced to optimize the resource usage of the data-driven models. The parallelization strategy involves distributing memory parallelism integrated according to the message passing interface (MPI) standard and shared memory parallelism with OpenMP at the computing node level for CPU-based platforms and heterogeneous programming with MPI/CUDA for platforms with a hybrid CPU-GPGPU architecture. Moreover, thanks to the flexibility of the ONNX runtime environment, ML models can run on both CPUs and GPGPUs.

Preliminary investigations of the library's performance were conducted in decaying homogeneous isotropic turbulence, and its performance was compared against widely-used models, such as the dynamic Smagorinsky model. To do so, a dedicated interface FORTRAN-C++ was implemented to exchange data between the in-house CFD code CIAO and the SuperLES library. The interface ensures timely data transfer at different stages of the simulation, maintaining efficiency and accuracy. The simulation performance and scalability were tested up to 64 GPU nodes. The SuperLES library showed good overall scalability with almost perfect scaling of model evaluation and negligible, compared to the calculation of the model predictions, CPU-GPU data transfer timings. This innovative approach for integrating data-driven models into CFD solvers holds significant potential to improve the predictive capabilities of turbulence closure models while preserving the scalability of the underlying CFD solver and allowing for control of computational resources, such as memory and performance required

by the ML framework that evaluates the data-driven models.

Acknowledgments The authors gratefully acknowledge the computing time granted by the NHR4CES Resource Allocation Board provided to them on the high-performance computer CLAIX at the NHR Center RWTH Aachen University. The computations for this research were performed using computing resources under project *rwth0658*. We thank Mr. R. Sedona and Dr. G. Cavallaro for their support in the porting of the application to DEEP-EST. The authors thank Prof. Antonio Attili, Mr. Fabian Fröde, and Mr. Christoph Schumann for their exceptional support and contributions to this research project.
The research leading to these results has received funding from the European Union's Horizon 2020 research and innovation program under the Center of Excellence in Combustion (CoEC) project, grant agreement no. *952181*, from the German Federal Ministry of Education and Research (BMBF), and the state of North Rhine-Westphalia for supporting this work as part of the NHR funding. The authors gratefully acknowledge the computing resources from the DEEP-EST project, which received funding from the European Union's Horizon 2020 research and innovation program under grant agreement no. *754304*.

Pohozhaev Identities and applications to the Generalized Solvability of One Nonlinear Problem of Mixed Type

N. Popivanov

We apply Pohozhaev type identity to boundary value problems for a mixed type equations with two orthogonal degeneration lines and power type nonlinearity. An overview of the established result for nonexistence of nontrivial regular solution of the problem is provided. We briefly discuss both supercritical and critical case. We outline the extension of the result for nonexistence of nontrivial regular solution to generalized solution. For this reason we prove a new results about Pohozhaev type identity for smooth functions. Discussing appropriate mollification operators in suitably localized domains we construct a sequence of smooth functions which approximate the generalized solution and finally use Pohozhaev type identity and Hardy-Sobolev inequality with remainder term to prove the nonexistence of nontrivial generalized solutions.
We will discuss some questions of existence of nontrivial solutions for a stronger type of degeneracy.

Solutions with exponential singularity for (3+1)-D Protter problems

T. Popov

We study some boundary-value problems for the wave equations that were proposed by Murray H. Protter in the context of models in fluid dynamics. In $\mathbb{R}^2$ the Guderley-Morawetz problem for the Gellerstedt equation of mixed hyperbolic-elliptic type is a classical model for transonic flows around airfoils. In the 1950s Protter proposed multi-dimensional analogues of the planar Guderley-Morawetz problem. Naturally, it was believed that one could adapt the methods used to study the planar case to attack the multi-dimensional problems. However, the the multi-dimensional Protter-Morawetz problem proved to be qualitatively different and the situation there is still not clear. Even the question of well-posedness is not completely resolved. In his analysis Protter considered some boundary-value problems not only in the mixed-type domains but also just in the hyperbolic part of the domain.

In the present talk we consider Protter's boundary-value problems for the nonhomogeneous wave equation in a domain, bounded by two characteristic cones and a non-characteristic ball. They can be regarded as a four-dimensional analogues of the Darboux problem in $\mathbb{R}^2$ – the boundary data are prescribed on one of the characteristic cones and the non-characteristic part of the boundary. Unlike the planar Darboux problem, in the framework of classical solvability, the Protter problem in $\mathbb{R}^4$ is not Fredholm. In fact, the homogeneous adjoint problem has an infinite number of linearly independent solutions. Alternatively, it is known that for smooth right-hand side functions, there is a uniquely determined generalized solution that may have a strong power-type singularity at one boundary point. The singularity is isolated at the vertex of the characteristic light cone and does not propagate along the cone, which makes this case different from the traditional case of propagation of singularity. For Protter problems with Neumann boundary condition on the non-characteristic part of the boundary, the behaviour of the generalized solution was studied in [1]. New singular solutions with exponential growth were announced in [2].

References

[1] N. Popivanov, T. Popov, A. Tesdall, Semi-Fredholm solvability in the framework of singular solutions for (3+1)-D Protter-Morawetz problem, *Abstract and Applied Analysis*, V. 2014, Article ID 260287, 1–19.

[2] N. Popivanov, T. Popov, I. Witt, Solutions with exponential singularity for (3+1)-D Protter problems, *Journal of Hyperbolic Differential Equations*, vol:20, issue:2, 2023, 475-498.

Mathematical modelling of laminar convective flows in water-flow glazing

M. Rashevski, S. Slavtchev

The report considers hydrodynamic and heat transfer processes occurring in a water-flow glazing exposed to sunlight, a subject of an innovative facade technology for reduced cooling needs and increased solar energy harvesting in buildings.

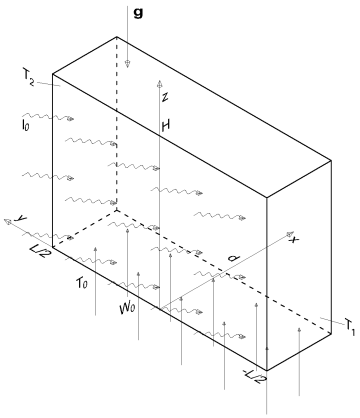

Figure 2: Scheme of rectangular duct

The glazing is modelled by a vertical duct of rectangular cross-section with two opposing transparent walls and the other two being opaque (Fig. 1). The study of natural and mixed convection in the duct is based on the Navier-Stokes equations in Boussinesq approximation and the energy equation with a heat source due to the light absorption in the water. The volumetric source induced by the solar radiation is described by the Beer-Lambert law:

$$Q = Q_0 e^{-\alpha x} \tag{22}$$

where Q_0 is the light source intensity at $x = 0$ and α is the optical depth. The flows are assumed well-developed and are characterized by constant pressure gradient along the duct and only one vertical velocity component being function of the coordinates x and y. Three combinations of temperature boundary conditions are studied: a case of isothermal walls with the heat source only and two cases of different temperatures on the transparent walls with linear distribution of the temperature on the lateral ones. In all cases the fluid is assumed cooler than the walls.

Analytical solutions of the governing equations are obtained as sums of the product of the sinus function and the hyperbolic functions. They are symmetric with respect to the medium

plane between the lateral walls. The natural and mixed convection depends on the Reynolds, Grashof and Prandtl numbers, the heat source intensity and the absorption properties in the near-infrared spectrum. Some important thermal characteristics of the flows such as the bulk liquid temperature and the Nusselt number are calculated. In the case of natural convection at equal wall temperatures, dimensionless velocity shapes are plotted in Fig. 2. for a quadratic cross-section duct and a rectangular duct with the aspect ratio of the sizes equal to 5. It is seen that in the central part of the rectangular duct the velocity profiles hardly change in the y-direction and are similar to each other.

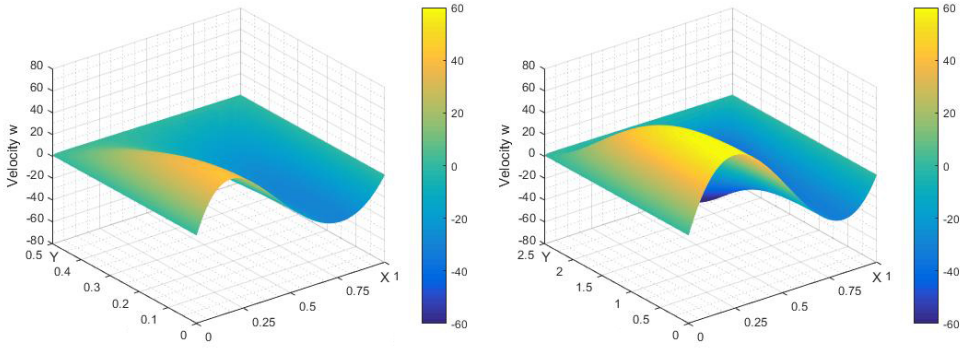

(a) (b)

Figure 3: Velocity fields in quadratic (3a) and rectangular (3b) ducts

It is found that when the aspect ratio is increased the velocity profiles and the thermal characteristics approximate those for flows in a flat channel fully confirming the results obtained in [1]. The main conclusion of the paper is that the developed mathematical model represents a good basis for accurate prediction of the flow behaviour and thermal characteristics in the water-flow glazing. It could be a potential tool for improvement and optimization of the aforementioned façade technology.

Acknowledgements The work is supported by the National Science Fund of Bulgaria under the program "Fundamental research for junior researchers and postdocs - 2022", grant: КП-06 ПМ62/3 /15.12.2022.

References

[1] M. Rashevski, S. Slavtchev, M. Stoyanova, Natural and mixed convection in a vertical water-flow chamber in the presence of solar radiation, Eng. Sc. and Tech., Int. J., Vol. 33, 101073, 2022

Aggregation energetics of putative linear AMPs: a case study

P. Sirakova, E. Lilkova, P. Petkov, N. Ilieva, L. Litov

Membrane-active peptides are promising biological molecules with possible applications in the treatment of various infection diseases. Within this class of small biological molecules, antimicrobial peptides (AMPs) attract the greatest research interest due to their broad-spectrum activity against a wide variety of pathogens and their potential application as a therapeutic alternative in the case of multi-drug resistant bacterial strains. AMPs exert their action by interacting with target cellular membranes, whereas they either insert into or penetrate the lipid bilayer. The physical quantity that governs the behaviour of molecular systems and the processes within them is the free energy. However, it is notoriously difficult to estimate reliably and accurately the free energy of biomolecular systems using standard molecular-dynamics (MD) simulations. This requires the application of advanced enhanced sampling techniques when estimation of the energetics of a biomolecular process is necessary.
Here we report the application of one such technique — the umbrella sampling, to estimate the binding energy between AMPs within peptide nanoclusters, thus evaluating the stability of this aggregates. The results show that the clusters are sufficiently stable and the aggregation process is practically irreversible in solution.

Acknowledgments This work was supported in part by the Bulgarian National Science Fund (Grant KP-06-OPR 03-10/2018). Computational resources were provided by the BioSim HPC Cluster at the Faculty of Physics at Sofia University "St. Kl. Ohridski", Sofia (Bulgaria) and by CI TASK (Centre of Informatics – Tricity Academic Supercomputer & networK), Gdansk (Poland).

Edge of chaos in integro-differential model of nerve conduction

A. Slavova, V. Ignatov

For dynamical systems in neuroscience, the type of bifurcation determines the computational properties of neurons. Neuronal models can be excitable for some values of parameters, and fire spikes periodically for other values. These two types of dynamics correspond to a stable equilibrium and a limit cycle attractor, respectively. When the parameters change, the models can exhibit a transition from one qualitative type of dynamics to another.
The most widely-used mathematical model of excitation and propagation of impulse (action potential) in nerve membranes is the Fitzhugh Nagumo equation [3]. It has been shown that this equation or the original Nagumo active pulse transmission can be unified under the umbrella of one or two-dimensional reaction-diffusion Cellular Nonlinear Networks (CNN) [2,5] where the cells are the degenerate case of Chua's oscillator. In our case, since the

Fitzhugh Nagumo equation is only a simplification of the classic Hodgkin-Huxley equations [4] for nerve conduction we shall prove that with the appropriate choice of circuit parameters CNN represents a more general and versatile model of nerve conduction.
We shall study the dynamics of the obtained CNN model via local activity theory [1]. Edge of chaos domain of the parameter set will be determined in the tow dimensional case [6]. Computer simulations will illustrate the obtained theoretical results. Some discussions on the complex behavior of the model of nerve conduction will be provided as well.

References

[1] L.O.Chua. Local Activity is the origin of complexity. Int.J.Bifurcation and Chaos,15:11, pp. 3435-3456, 2005.
[2] L.O. Chua, L.Yang, Cellular Neural Networks, Theory and Applications, IEEE TCAS-I, 1988
[3] R. FitzHugh, Impulses and physiological states in theoretical models of nerve membrane,Biophysics. J., 1, (1961): 445–466.
[4] A. L. Hodgkin and A. F. Huxley, A quantitative description of membrane current and its application to conduction and excitation in nerve, J. Physiology, vol. 117 (1952): 500–544.
[5] A. Slavova. Cellular Neural Networks:Dynamics and Modeling, Kluwer Academic Publishers, 2003.
[6] A.Slavova, R. Tetzlaff. Edge of chaos in reaction diffusion CNN model. Open Mathematics, 15:1, 2017.

Influence of Wide Focus Attention Semantic Prime on Volitional Saccades of Two Adult Groups During Evaluation Detailed of Colourfull Photos Forming Aesthetic Perceptions

M. Staneva, M. Iliev, I. Sazdova, H. Gagov, T. Dimitrova, T. Dimitrov

Saccades provide useful information for the momentary attention, because shifts of the gaze are preceded by a deviation of attention [1, 2]. The unconscious activation of cognitive processes before the performance of various tasks is a phenomenon with strong impact on people's cognition [3]. This method is called semantic priming [4, 5, 6, 7]. The present work studies the influence of semantic priming on the characteristics of voluntary saccades during visual image analysis of participants divided in groups by gender and age.
Participants seated 65 cm from a 31-inch screen with a resolution of 1366 x 768 pixels and their heads were fixed in chin-rest. Eye movements were recorded using an Eye Tracker GP3HD at 150 Hz. Python program extracted the eye movement parameters: i) saccade duration; ii) the latency of the first saccade; iii) saccade amplitude and iv) fixation duration. After delay of 3 seconds (sec) (appearance of a fixation target), photos appeared on the entire screen. The presentation of each image lasted 20 sec. The presentation consisted of 16 photos. The participants were instructed to examine the images in detail and to detect differences in the two halves of the visual space. The people from Control group only viewed 16

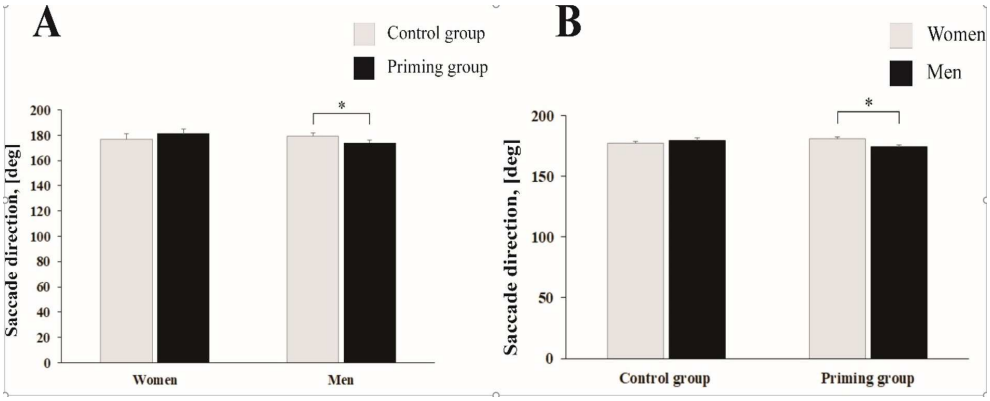

Figure 4: Gender differences in median saccade direction. A, right panel: In men group priming test significantly reduced median saccade direction vs Control group. B, right panel: The priming test had stronger effect in men group compared to women.

photos, while the participants in Priming group first wrote Priming test for wide focus and then viewed these pictures. Data are expressed as mean $\pm$ standard error of the mean (SEM). The difference between Control group and Priming group was tested by Student's t-test for independent samples. A value of p ¡ 0.05 was considered significant.

Twenty-four healthy people aged from 47 to 75 years took part in the study. Mean age of Control group was 56.88 ± 1.59 years and of Priming Group - 55.8 ± 1.4 years. Gender-dependent differences in the median saccade direction were observed as a result of Priming test. In men the median saccade direction in Control vs Priming group was reduced by $4,99 \pm 1,69$ degree (deg) (p¡0.05; Fig. 1A) while in women the median saccade direction was not changed significantly. It increased with $4,42 \pm 4,16$ deg (p=0.658; Fig. 1A). It was also observed gender difference in Priming group (Fig. 1B). The priming test reduced the median saccade direction in men group compared to women with $7,04 \pm 2,57$ deg (p¡0.05; Fig. 1B), while in Control group the median saccade direction increased with $2,19 \pm 1,82$ deg (p=0.371; Fig 1B).

It is concluded that the application of priming test with wide focus of attention on visual elements in separate parts of the visual field reduces the median saccade direction in male group. The observed change of median saccade direction suggests a moderate influence of semantic priming on cognitive function.

Acknowledgement This research was funded by grant FNI-KP-06-M-43/4 from the Scientific Research Fund of the Ministry of Education and Science of Bulgaria.

References

[1] Braun, D. I., Alexander C., Schütz A. C., Gegenfurtner K. R. Age effects on saccadic suppression of luminance and color. J. Vision. 21, 11 (2021).

[2] Chavant, M., Kapoula, Z. Loss of audiovisual facilitation with age occurs for vergence eye movements but not for saccades. Sci. Rep. 12, 4453 (2022).

[3] Petracca, E. Two and a half systems: The sensory-motor system in dual-process judgment and decision-making. J. Neurosci. Psychol. Economics. 13, 1-18 (2020).
[4] Bargh, J. A. The Historical Origins of Priming as the Preparation of Behavioral Responses: Unconscious Carryover and Contextual Influences of Real-World Importance. Soc. Cognition 32(Suppl.), 209-224 (2014).
[5] Bock, O., Grigorova, V., Ilieva-Staneva,M. Adaptation of Reactive Saccades is Influenced by Unconscious Priming of the Attention Focus. J. Mot. Behav. 49, 477-481 (2017).
[6] Bock, O., Grigorova, V., Ilieva, M. Double-Step Adaptation of Saccadic Eye Movements Is Influenced by Priming with Age Stereotypies. Psychol. 12, 1014-1017 (2013).
[7] Staneva, M., Grigorova, V., Bock, O. Semantic priming for attention focus influences visuomotor tasks differently but the Effects are Similar in Young and Older Adults. J. Mot. Behav. 51, 580-586 (2019).

External Validation of Paraphrasing Language Models with Respect to Bulgarian

T. Stefanova, T. Georgiev

In the recent years large language models (LLMs) are becoming more and more popular and their usage is tremendously increasing. These models can perform various tasks, and a lot of them are related to text generation.
One of the most important aspects of a machine learning model is how well it works. There are two main ways of validating such models. One is internal – in this case authors split all of the data they use in three parts (the so-called train-test-validation split). The train and test parts are used during the training stage and the validation part is for evaluation after the model is trained. The other way is external (or independent). It is done using another dataset and often by independent researchers who have not participated in training the model. Usually such validation is done in order to prove the robustness and scalability of the model.
When talking about large language models, most of their authors claim some overall performance, but do not always evaluate the different tasks their models can complete and are rarely specific about the performance in a concrete language. Another serious gap is that very little research and very little external validation of such models has been conducted about text generation in a specific language, especially in Bulgarian. This is what our study is about. We have chosen a task which provides a pivot for our expectations about the generated text, namely paraphrasing. This task is very similar to machine translation when it comes to the technical side of its validation as pairs of input text and expected output text are needed. The difference is that paraphrasing requires the input and the output text to be in the same language. For this reason we have chosen to use two public datasets - TaPaCo and the Cross-lingual Natural Language Inference (XNLI).
TaPaCo is a dataset containing paraphrases in 73 languages extracted from the Tatoeba database which relies on crowdsourcing for the translation of phrases in different languages.
XNLI is a dataset created by manually translating the test and validation sets of the Multi-genre NLI corpus to 15 languages and adding the machine translation to the same 15 lan-

guages of the train set.
The models, subject to external validation in this research, are OpenAI's GPT-3, BigScience's BLOOM, Meta's LLaMA 2 and XGLM.
Apart from the traditional metrics used for classification tasks, which authors of LLMs usually provide, such as accuracy, precision, F1-score and recall, there are other metrics for language generating tasks. Some of them, used in this work for evaluating the above-mentioned models, are BLEU (BiLingual Evaluation Understudy), ROUGE (Recall-Oriented Understudy for GistingEvaluation), METEOR (Metric for Evaluation of Translation with Explicit ORdering) and WER (Word-Error Rate).
The methodology used for evaluating paraphrasing performance is similar to that of machine translation as the same metrics are usually applied, but while translation has low tolerance to versatility of the words and phrases used in the output, sentences can be paraphrased in much more ways and it depends on the particular purpose of paraphrasing, e.g. summarizing, expanding, changing the style, and many more.

Sensitivity Analysis of a Large-Scale Air Pollution Model by Highly Efficient Lattice Generating Vectors

V. Todorov, S. Georgiev

Mathematical modeling is a powerful approach that involves the creation of mathematical structures to represent, analyze, and understand real-world phenomena. It is a fundamental tool across various scientific disciplines and industries, providing a systematic way to describe complex systems and their behaviors. In mathematical modeling, relationships, patterns, and interactions within a given system are translated into mathematical equations or algorithms, enabling the exploration of scenarios, predictions, and decision-making. This process allows researchers, engineers, and scientists to gain insights into the underlying principles governing natural and artificial processes, facilitating the optimization of solutions, identification of trends, and the development of strategies for problem-solving and innovation. Mathematical modeling plays a crucial role in advancing scientific knowledge, aiding in the design of experiments, simulations, and the formulation of hypotheses, ultimately contributing to the advancement of technology and our understanding of the world.
Sensitivity analysis [1] is a critical component of mathematical modeling, providing valuable insights into the robustness, reliability, and responsiveness of a model's predictions to variations in input parameters. It assesses the impact of uncertainties in the model's parameters on the outcomes, thereby enhancing the model's credibility and usefulness. In mathematical modeling, where real-world systems are often characterized by inherent variability and imprecision, sensitivity analysis helps identify influential factors and their contribution to the model's outputs. This process enables modelers to focus on refining key parameters, improving the model's accuracy, and making informed decisions based on a thorough understanding of potential uncertainties. Sensitivity analysis [2] is indispensable in guiding model calibration, validation, and ensuring the model's adaptability to diverse scenarios. By systematically exploring the effects of parameter variations, sensitivity analysis enhances the model's

applicability, aids in risk assessment, and contributes to the overall reliability of mathematical models across various fields, including science, engineering, finance, and environmental studies.

Monte Carlo methods [3] hold significant importance in sensitivity analysis within mathematical modeling. Sensitivity analysis aims to assess the impact of variations or uncertainties in input parameters on the model's output. In this context, Monte Carlo simulations serve as a powerful tool to explore the sensitivity of a mathematical model to changes in input variables.

Lattice rules are deterministic point sets designed to achieve a more uniform distribution of points compared to traditional Monte Carlo methods and play a crucial role within these methods, contributing significantly to the accuracy and efficiency of simulations. Traditional random sampling techniques can exhibit irregularities or clustering, leading to suboptimal convergence rates and increased variance in Monte Carlo estimates. Lattice rules address this issue by employing a systematic arrangement of points in multidimensional space, often forming a lattice or a grid. These quasi-random sequences offer a more evenly distributed set of points, reducing the discrepancy and improving the coverage of the sample space.

The importance of lattice rules lies in their ability to enhance the efficiency of Monte Carlo simulations, particularly in high-dimensional problems. Quasi-random sequences generated by lattice rules produce a more uniform exploration of the input space, leading to faster convergence and, consequently, more accurate estimates of integrals or solutions to mathematical problems.

The Unified Danish Eulerian Model (UNI-DEM) [4] is an advanced atmospheric chemistry transport model that has been widely used for studying air quality, pollutant dispersion, and atmospheric chemistry. Developed by the National Environmental Research Institute of Denmark (NERI), UNI-DEM integrates various components of atmospheric processes, allowing for a comprehensive understanding of the dynamics and interactions influencing air quality.

One of the notable features of UNI-DEM is its ability to simulate the transport and transformation of pollutants over a range of spatial and temporal scales. It incorporates detailed representations of emission sources, atmospheric dispersion, chemical reactions, and deposition processes. This holistic approach enables researchers to assess the impact of emissions from both local and distant sources on air quality in a given region.

Generating vectors for lattice rules is a crucial aspect of quasi-Monte Carlo (QMC) methods, which are employed for numerical integration and sampling in high-dimensional spaces. The generation of vectors for lattice rules involves careful construction to ensure desirable properties such as low discrepancy and improved convergence rates.

In this work we will make a special choice of the generating vectors. This choice of a specific method for generating vectors depends on the application, dimensionality of the problem, and the desired properties of the lattice rule. We will explore different constructions and sequences to find the most suitable approach for a particular numerical integration.

In summary, in this paper we will deploy highly efficient generating vectors for lattice rules for evaluating the sensitivity indices obtained through sensitivity analysis with respect to emission levels and chemical reaction rates of the Unified Danish Eulerian model.

Acknowledgement This work is supported by the BNSF under Project KP-06-M62/1 "Numerical deterministic, stochastic, machine and deep learning methods with applications in

computational, quantitative, algorithmic finance, biomathematics, ecology and algebra" from 2022.

References

[1] A. Saltelli, Tarantola, S., Campolongo, F., Ratto,M.: Sensitivity Analysis in Practice: A Guide to Assessing Scientific Models. Halsted Press, New York (2004).

[2] I. T. Dimov, R. Georgieva. Multidimensional Sensitivity Analysis of Large-scale Mathematical Models, Springer Proceedings in Mathematics & Statistics 45, Springer Science+Business Media, New York, 2013, 137–156.

[3] I.T. Dimov, Monte Carlo Methods for Applied Scientists, New Jersey, London, Singapore, World Scientific (2008), 291 p., ISBN-10 981-02-2329-3.

[4] Z. Zlatev, I. T. Dimov, Computational and Numerical Challenges in Environmental Modelling, Elsevier, Amsterdam, 2006.

Is Molecular Mimicry a Player in SARS-CoV-2 Successful Cell Invasion?

N. Todorova, M. Rangelov, P. Petkov, C. Nedeva, E. Lilkova, N. Ilieva, L. Litov

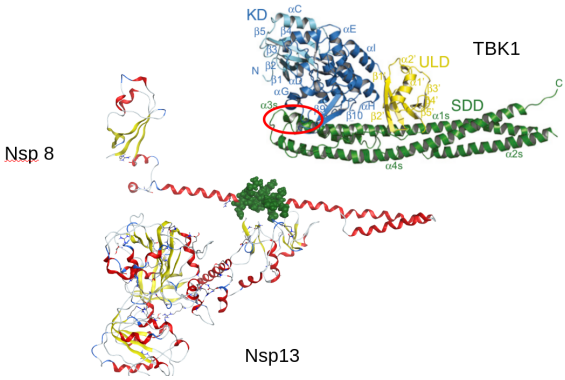

SARS2-CoV machinery is extremely complex, with most proteins playing multiple roles in viral cell cycle. Interaction with host antiviral defense mechanisms form a network, with one focus in interferon type I activation blockage. Based on molecular model of replicase-transcriptase complex of the virus, starting with XRD 7CYQ, we found evidence for sequencial and structural similarity between viral protein and eukaryotic protein, involved in interferone type I activation pathway. After molecular dynamics of the multiprotein viral complex, we inspected molecular contacts of involved in the complex non structural proteins (nsp7, nsp8, nsp12, nsp13), especially those between nsp8 and nsp13. TANK-binding kinase 1 (TBK1) is part of interferon I activation and we suspected similarity with nsp8, that was

further explored. We searched with appropriate algorithm for similarities between all possible fragments, 10 aa in length or longer, from the sequence of nsp8 (7CYQ) and they were aligned and compared in all possible positions to TBK1 sequence (4IWO) in accordance with similarity matrices: BLOSUM45, BLOSUM62, BLOSUM80 and BLOSUM90. This strategy could overcome the problem with the lack of common ancestor between viral and eukaryotic protein. The most promising fragment contained 11 aa and beside high sequential similarity posses also similar secondary structure in both proteins (helix). This fragment was situated in nsp8 exactly where it contacts with nsp13. Therefore we hypothesized that place as an important for probable suppression of TBK1 function and in such activation of interferon I pathway. Guo et al. 2021 report that "nsp13 might suppress type I interferon production through interacting with TBK1", where our finding is that nsp13 probably interacts with TBK1 in a region, similar to nsp8. Moreover they found that SDD (scaffold dimerization domain) is required for the interaction of TBK1 and nsp13, but without any further assumption. Where we found the molecular reason for this finding: the similarity between nsp8 and TBK1 is exactly in the SDD domain of TBK1. SDD domain is crucial for TBK1 dimerization needed for its normal function. Further molecular dynamic simulation of TBK1 and nsp13 simulation shows interaction in the aa sequence of TBK1, found already as the most similar to nsp8. As our findings represent nsp8 is similar to TBK1, we propose a hypothesis for blocking IFN type 1 activation pathway. Either 1) nsp8 interferes with TBK1 activation, preventing its dimerization or 2) nsp13 binds to TBK1 or both of them. As in the literature there are in vitro tests, that could confirm both statements, more experiments targeting involved molecules are needed in order to shed light on that part of viral proteins function.

Acknowledgments This research was partially funded by the Bulgarian National Science Fund under Grant KP-06-DK1/5/2021 SARSIMM. Computational resources were provided by the Discoverer supercomputer thanks to Discoverer PetaSC and EuroHPC JU, as well as the BioSim HPC cluster at the Faculty of Physics, Sofia University "St. Kliment Ohridski".

Point-cyclic $KTS(45)$

S. Topalova, S. Zhelezova

A Steiner triple system of order v ($STS(v)$) is a pair (V, B) where V is a v-element set and B is a family of 3-element subsets of V called blocks such that each pair of elements of V is contained in exactly one block of B. There are $b = v(v-1)/6$ blocks and each point is in $r = (v-1)/2$ blocks.
A parallel class is a partition of the point set by blocks. There are v/k blocks in each parallel class. A resolution of an $STS(v)$ is a partition of the collection of blocks to parallel classes. An $STS(v)$ together with a resolution of its blocks is called a Kirkman triple system ($KTS(v)$).
$KTS(v)$ are related to error correcting codes in many different ways. It is well known that a $KTS(v)$ is equivalent to an optimal $(r, 3q, r-1)_q$ equidistant code [1]. We consider

$KTS(45)$. They are $KTS(v)$ with $v \equiv 9 \ (mod \ 18)$. These $KTS(v)$ are used in constructions of asymptotically optimal erasure-resilient codes for large disk arrays that can tolerate failures [2]. Very recently $KTS(v)$ are involved in constructions of Protograph LDPC Codes for a Block Fading Channel [3].

A $KTS(v)$ exists iff $v \equiv 3 \ (mod \ 6)$, $v \geq 3$ [4]. General constructions of $KTS(v)$ are presented in [5,6]. $KTS(v)$ are completely classified only up to $v = 15$ [7,8]. Many authors construct $KTS(v)$ with $v > 15$ and with prescribed automorphisms or with subsystems. One of the most recent results is on $KTS(21)$ and presents over 13 million $KTS(21)$ with subsystems $STS(7)$ and $STS(9)$ [9]. The full classification of $KTS(21)$ is out of reach now. A $KTS(45)$ with $STS(21)$ as a subdesign can be obtained from the infinite class of $KTS(2u + 3)$ with $STS(u)$ as a subdesign [10].

An $STS(v)$ is cyclic if it has a cyclic automorphism group of order v. There is a one-to-one correspondence between cyclic $STS(v)$ and $(v, k, 1)$ cyclic difference families. The blocks of a cyclic $STS(v)$ are partitioned under the automorphism group of order v to $(v - 3)/6$ block orbits of length v and one short block orbit of length $v/3$. A cyclic $STS(v)$ is cyclically resolvable if it has a resolution with an automorphism permuting the points in one cycle. Such a resolution is called point-cyclic. Only cyclic $STS(v)$ can have point-cyclic $KTS(v)$.

General constructions of point-cyclic $KTS(v)$ are considered in [11,12]. All point-cyclic $KTS(21)$ and $KTS(39)$ are presented in [13] and $KTS(27)$ in [14]. The next open case is the classification of point-cyclic $KTS(45)$ which we consider in this work.

All the 11616 cyclic $STS(45)$ are known [15], but the classification of all their resolutions is a computationally difficult problem, because of the very big number of parallel classes comprising a particular triple.

In this work we succeed to construct all nonisomorphic point-cyclic $KTS(45)$. Their number is 2128. The short block orbit of the cyclic $STS(45)$ is a parallel class in all point-cyclic $KTS(45)$. For all the constructed $KTS(45)$ we compute the order of the automorphism group and establish some additional properties which are of interest for their possible applications.

Acknowledgemnts Partially supported by the Bulgarian National Science Fund under Contract No KP-06-H62/2-2022.

References

[1] N. V. Semakov, V. A. Zinovev. Equidistant q-ary codes with maximal distance and resolvable balanced incomplete block designs (in Russian), Problemy Peredachi Informatsii 4 (1968) 3–10. English translation in Problems Inform. Transmission 4 (1968) 1–7.

[2] Y. M. Chee, C. J. Colbourn, A. C. H. Ling. Asymptotically optimal erasure-resilient codes for large disk arrays, Discrete Appl. Math., 102 (1–2) (2000) 3–36.

[3] J. Kim, C. Kim, H. Park, J. -S. No. Design of Protograph LDPC Codes Using Resolvable Block Designs for Block Fading Channel," in IEEE Wireless Communications Letters, vol. 11, no. 9, 2022, pp. 1970-1974.

[4] D.K.Ray-Chaudhuri, R.M.Wilson. Solution of Kirkman's school-girl problem, Proc. Sympos. Pure Math. 19, Amer. Math. Soc., Providence, R.I., 1971, pp. 187–203.

[5] X. -Y. Li, Z. -D. Xu, W. -X. Chou. A new method of constructing Kirkman triple system, 2011 Chinese Control and Decision Conference (CCDC), Mianyang, China, 2011, pp. 4237-4242.

[6] D.R. Stinson. A survey of Kirkman triple systems and related designs, Discrete Math, 92 (1–3) (1991) 371–393.
[7] F. N. Cole. Kirkman Parades, Bull. Amer. Math. Soc. 28 (1922) 435-437.
[8] P. Mulder. Kirkman-systemen, PhD Thesis, Rijksuniversiteit Groningen, 1917.
[9] J. I. Kokkala, P. R.J. Östergård. Kirkman triple systems with subsystems, Discrete Math, 343 (9) (2020) article: 1111960.
[10] P. J. Dukes, E. R. Lamken. An update on the existence of Kirkman triple systems with Steiner triple systems as subdesigns, J Comb Des, 30 (8)(2022) 581–608.
[11] M. Genma, M. Mishima, M. Jimbo, Cyclic resolvability of cyclic Steiner 2-designs, J. Combin. Des. 5 (3) (1997) 177–187.
[12] M. Mishima, M. Jimbo. Recursive constructions for cyclic quasiframes and cyclically resolvable cyclic Steiner 2-designs, Discrete Mathematics 211 (1) (2000) 135–152.
[13] C. W. H. Lam, Y. Miao. Cyclically resolvable cyclic Steiner triple systems of order 21 and 39, Discrete Math, 219 (1-3) (2000) 173–185.
[14] C. J. Colbourn, S. S. Magliveras, R. A. Mathon. Transitive Steiner and Kirkman triple systems of order 27, Math Comput 58 (197) (1992) 441–449.
[15] C.J. Colbourn & A. Rosa, Triple Systems, Clarendon Press, Oxford, 1999.

Exact solutions to a class of complex Ginzburg-Landau equations

V. Vassilev

Various processes and phenomena studied within the theory of phase transitions, nonlinear optics (wave propagation in optical fibers), electrical transmission lines, laser physics, fluid mechanics, and many other branches of physics, are modelled on the ground of complex Ginzburg-Landau equations, which capture dispersive and nonlinear effects. The foregoing equations may be thought of as generalizations of the standard nonlinear Schrödinger equation. In this talk, I will present, in analytic form, new exact solutions to certain classes of equations of the aforementioned type, which represent different kinds of solitary waves. These solutions are obtained using the Lie transformation group theory and the method of differential constraints.

Modeling Information Security Management System (ISMS) with Neural Networks (NN)

T. Velev, N. Dobrinkova, M. Veleva

An Information Security Management Systems (ISMS) are essential frameworks of policies, procedures and documents that organizations employ to manage and protect their information assets. These systems encompass people, processes, and technology to establish, implement, monitor, review, and maintain information security within an organization. The primary goal

of an ISMS is to ensure the confidentiality, integrity, and availability of information assets. ISMS are often based on international standards such as ISO/IEC 27001, which provides a framework for establishing, implementing, maintaining, and continually improving an information security management system. Implementing an ISMS requires a holistic and ongoing effort from the entire organization. It's not only a technical solution but also involves the active participation of employees at all levels and a commitment to a culture of security.

Modeling Information Security Management System (ISMS) with neural algorithms is an emerging field that has the potential to revolutionize the way organizations manage information security. NN are a type of artificial intelligence that can be used to automate certain tasks, improve decision-making processes, and provide more effective security measures.

The article represents an approach to making ISMS live by using neural networks for ongoing audit, monitoring, control, self-assessment and self-improvement. The model is based on artificial intelligence management of security controls and their attributes – types, security properties, capabilities, cybersecurity areas and security domains. Using the best practices controls are classified into 4 categories: people, if they concern individual people; physical, if they concern physical objects; technological, if they concern technology; and organizational. For different groups are appropriate different neural algorithms.

For different groups are appropriate different neural algorithms. Mainly applicable are: Feedforward Neural Network (FNN), including Multilayer Perceptions (MLPs) networks; Recurrent Neural Network (RNN), including Echo State Network (ESN), suitable for tasks with the sequence of input data such as time series analysis; Radial Basis Function Network (RBFN), three layers network for pattern recognition and function approximation; Hopfield Network, for associative memory and optimization problems; Boltzmann Machine; and Transformers

The prerequisite for automation using neural networks is the use of integrated information system managing the digital operational processes and documents of ISMS. The system have to digitizes, registers, manages, stores and controls work processes and related information and documentation, in accordance with a ISMS.

Neural algorithms and machine learning techniques are applied in various ways in many areas in the information and cyber security such as: Intrusion Detection Systems (IDS); Malware Detection; User Authentication and Access Control; Threat Intelligence and Information Security; Network Security; Automated Firewall Rule Optimization; Security Monitoring and Incident Response; Security Information and Event Management (SIEM); Phishing Detection; URL Analysis; Behavior-Based Endpoint Protection; Vulnerability Management; User Behavior Analytics; and many others. However for Information Security Management Systems as a whole Neural Networks are a new approach to provide huge increases in the effectiveness and efficiency, to reduce costs and time, and prevent or mitigate the damage. Generate the basis for making informed decisions about how to allocate the resources and to improve the overall security posture of organization.

Formulae in Closed Form for Subdivision of Bézier Surfaces using the Blossoming Principle

K. Vlachkova

We consider the problem of Bézier surfaces subdivision using blossoming and present two formulae in closed form that are more suitable for evaluation of the corresponding control points.

For any polynomial surface patch $S(u,v) = \sum_{i=0}^{n}\sum_{j=0}^{m} \mathbf{c}_{ij}u^iv^j$ of degree (n,m) defined for $a \le u \le b$ and $c \le v \le d$, the Bézier control points $\mathbf{p}_{\nu\mu}$, $\nu = 0,\dots,n$, $\mu = 0,\dots,m$, of this surface patch are (see [1])

$$\mathbf{p}_{\nu\mu} = b^{\square}(\underbrace{a,\dots,a}_{\nu},\underbrace{b,\dots,b}_{n-\nu},\underbrace{c,\dots,c}_{\mu},\underbrace{d,\dots,d}_{m-\mu}), \tag{23}$$

where

$$b^{\square}(u_1,\dots,u_n,v_1,\dots,v_m) = \sum_{i=0}^{n}\sum_{j=0}^{m} \mathbf{c}_{ij}b_{ij}^{\square}(u_1,\dots,u_n,v_1,\dots,v_m)$$

is the blossom of $S(u,v)$, and

$$b_{ij}^{\square}(u_1,\dots,u_n,v_1,\dots,v_m) = \sum_{\{\alpha_1,\dots,\alpha_i\}\subseteq\{1,\dots,n\}} \frac{u_{\alpha_1}\dots u_{\alpha_i}}{\binom{n}{i}} \sum_{\{\beta_1,\dots,\beta_j\}\subseteq\{1,\dots,m\}} \frac{v_{\beta_1}\dots v_{\beta_j}}{\binom{m}{j}} \tag{24}$$

is the blossom of the monomial u^iv^j. In the case where either $i = 0$, or $j = 0$, the corresponding sum in (24) equals 1, e. g. $b_{00}^{\square} = 1$. Here we establish formula (24) in an equivalent closed form that is more suitable for computations.

Theorem 1 *Bézier control points* $\mathbf{p}_{\nu\mu}$, $\nu = 0,\dots,n$, $\mu = 0,\dots,m$, *defined by (23) are* $\mathbf{p}_{\nu\mu} =$

$$\sum_{i=0}^{n}\sum_{j=0}^{m} \frac{\mathbf{c}_{ij}}{\binom{n}{i}\binom{m}{j}} \sum_{k=\max(0,i+\nu-n)}^{\min(i,\nu)} \sum_{r=\max(0,j+\mu-m)}^{\min(j,\mu)} \binom{\nu}{k}\binom{n-\nu}{i-k}\binom{\mu}{r}\binom{m-\mu}{j-r} a^k b^{i-k} c^r d^{j-r}.$$

□

For any polynomial surface path $S(u,v) = \sum_{i=0}^{n}\sum_{j=0}^{m} \mathbf{c}_{ij}u^iv^j$ of total degree $n+m$ defined in a triangle $\triangle MNP$, the Bézier control points $\mathbf{q}_{\nu\mu}$ of this surface patch are (see [1])

$$\mathbf{q}_{\nu\mu} = b^{\triangle}(\underbrace{M,\dots,M}_{\nu},\underbrace{N,\dots,N}_{\mu},\underbrace{P,\dots P}_{n+m-\nu-\mu}), \tag{25}$$

where

$$b^{\triangle}((u_1,v_1),\dots,(u_{n+m},v_{n+m})) = \sum_{i=0}^{n}\sum_{j=0}^{m} \mathbf{c}_{ij}b_{ij}^{\triangle}((u_1,v_1),\dots,(u_{n+m},v_{n+m}))$$

is the blossom of $S(u,v)$, and

$$b_{ij}^{\triangle}((u_1,v_1),\ldots,(u_{n+m},v_{n+m})) = \sum_{\substack{\{\alpha_1,\ldots,\alpha_i\}\subseteq K \\ \{\beta_1,\ldots,\beta_j\}\subseteq K\setminus\{\alpha_1,\ldots,\alpha_i\}}} \frac{u_{\alpha_1}\ldots u_{\alpha_i} v_{\beta_1}\ldots v_{\beta_j}}{\binom{n+m}{i,j}}, \quad (26)$$

$K=\{1,\ldots,n+m\}$, $\binom{n+m}{i,j}=\frac{(n+m)!}{i!j!(n+m-i-j)!}$, is the blossom of the monomial $u^i v^j$. In the case where either $i=0$, or $j=0$ the corresponding sum in (26) equals 1. Similar to the case of tensor product Bézier surfaces we present formula (25) in an equivalent closed form that is more suitable for evaluations of the control points.

Theorem 2 *Bézier control points* $\mathbf{q}_{\nu\mu}$, $\nu=0,\ldots,n$, $\mu=0,\ldots,m$, *defined by (25) are* $\mathbf{q}_{\nu\mu}=\sum_{i=0}^{n}\sum_{j=0}^{m}\frac{\mathbf{c}_{ij}}{\binom{n+m}{i,j}}b_{ij}^{\triangle}=$

$$\sum_{j_\beta=\underline{j}_\beta}^{\bar{j}_\beta}\sum_{j_\alpha=\underline{j}_\alpha}^{\bar{j}_\alpha}\sum_{i_\beta=\underline{i}_\beta}^{\bar{i}_\beta}\sum_{i_\alpha=\underline{i}_\alpha}^{\bar{i}_\alpha}\binom{\nu}{i_\alpha}\binom{\mu}{i_\beta}\binom{\lambda}{i_\gamma}\binom{\nu-i_\alpha}{j_\alpha}\binom{\mu-i_\beta}{j_\beta}\binom{\lambda-i_\gamma}{j_\gamma}a_1^{i_\alpha}b_1^{i_\beta}c_1^{i_\gamma}a_2^{j_\alpha}b_2^{j_\beta}c_2^{j_\gamma},$$

where

$$\begin{aligned}
&\lambda=n+m-\nu-\mu,\ i_\gamma=i-i_\alpha-i_\beta,\ j_\gamma=j-j_\alpha-j_\beta,\\
&\underline{i}_\alpha=\max(0,i-\mu-\lambda),\ \bar{i}_\alpha=\min(i,\nu),\\
&\underline{i}_\beta=\max(0,i-\nu-\lambda),\ \bar{i}_\beta=\min(i-i_\alpha,\mu),\\
&\underline{j}_\alpha=\max(0,j-(\mu-i_\beta)-(\lambda-i_\gamma)),\ \bar{j}_\alpha=\min(j,\nu-i_\alpha),\\
&\underline{j}_\beta=\max(0,j-(\nu-i_\alpha)-(\lambda-i_\gamma)),\ \bar{j}_\beta=\min(j-j_\alpha,\mu-i_\beta).
\end{aligned}$$

□

Acknowledgments This work was supported in part by Sofia University Science Fund Grant No. 80-10-103/2023.

References

[1] Goldman, R., *Pyramid algorithms: A dynamic programming approach to curves and surfaces for geometric modeling*, 2003, Elsevier Science (USA).

Finite element analysis of impact response of laminated glass

Z. Zhelev, M. Datcheva

The focus of this study is predicting the damage response of laminated glass to impacts. Laminated glass comprises a polymer composite with brittle outer layers and a soft inner

layer. The structure is recognized as safety glass due to its capacity to absorb impact energy effectively and to securely bond glass fragments.
The analyses are performed by the finite element method. All numerical results are obtained in the LS-DYNA environment, which is an industry-leading explicit simulation software widely recognized for its application in impact simulations.
The loading scenario is a pendulum test on a glass structure, as outlined in EN 12600:2003. The numerical model is simplified, with the emphasis placed on glass modeling. In the performed simulations, the ball moves perpendicularly to the glass structure with a given initial velocity.

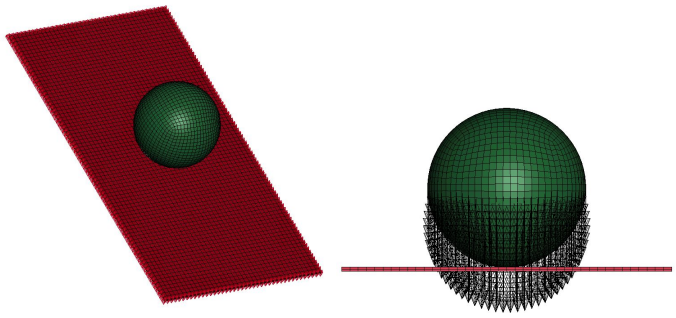

(a) General view of the ball and the target with its supported edges

(b) Direction of the initial velocity of the ball

Figure 5: Model of impact simulation

The theoretical basis of the Johnson-Holmquist II constitutive model, designed for brittle materials subjected to significant strains, high strain rates, and elevated pressures, is briefly discussed. Instead of explicitly modeling individual cracks, glass material is treated as if it contains distributed voids (isotropic damage), represented by a variable that adopts values between 0 and 1. As damage evolves the strength of the material decreases.
The algorithm utilized for implementing the Johnson-Holmquist II (JH2) in the finite element code is also discussed.
Despite the fact that there are other numerical approaches that yield more accurate results for analyzing impact mechanics problems, the implementation of JH2 coupled with element erosion technique is an approach that works good for engineering purposes. It achieves good balance between accurate representation of the mechanical phenomenon and maintaining degree of computational efficiency.
Furthermore, the influence of different constitutive and model parameters is studied. Different techniques for modelling the ball are compared. A study on the impact of refinement of the finite-element discretization is performed and the finite element shape and size are analyzed. Different methods for fixing the PVB plug in the glass construction are compared. Finally, the influence of the damage parameter on the response of the glass construction is investigated.

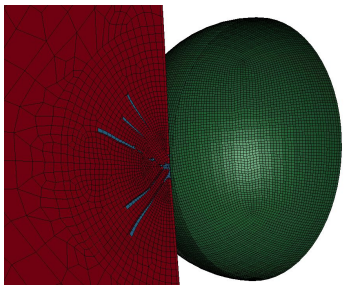

Figure 6: Computed damage zones results of the analysis of the structure with mesh in radial direction

Acknowledgments The work is supported by the National Science Fund of Bulgaria under the program "Fundamental research for junior researchers and postdocs - 2022", grant: KP-06 PM62/3 /15.12.2022.
Special thanks to Mott MacDonald Bulgaria who provided access to the LS-DYNA software that made this study possible.

Part B

List of participants

Todorka Alexandrova
Institute of Mathematics and Informatics
Bulgarian Academy of Sciences
Acad. G. Bonchev Str., Bl. 8
1113 Sofia, Bulgaria
toty@math.bas.bg

Hristo Chervenkov
National Institute of Meteorology
and Hydrology
Boulevard "Tsarigradsko shose" 66,
1784 7-Mi Kilometar,
Sofia, Bulgaria
hristo.tchervenkov@meteo.bg

Maria Datcheva
Institute of Mechanics
Bulgarian Academy of Sciences
Acad. G. Bonchev Str., Bl. 4
1113 Sofia, Bulgaria
datcheva@imbm.bas.bg

Nina Dobrinkova
Institute of Information and
Communication Technologies
Bulgarian Academy of Sciences
Acad. G. Bonchev Str., Bl. 25A
1113 Sofia, Bulgaria
ninabox2002@gmail.com

Stefka Fidanova
Institute of Information and
Communication Technologies
Bulgarian Academy of Sciences
Acad. G. Bonchev Str., Bl. 25A
1113 Sofia, Bulgaria
stefka.fidanova@gmail.com

Georgi Gadzhev
National Institute of Geophysics,
Geodesy and Geography
Bulgarian Academy of Sciences, Acad. G.
Bonchev Str., Bl. 3,
1113 Sofia, Bulgaria
ggadjev@geophys.bas.bg

Kostadin Ganev
National Institute of Geophysics,
Geodesy and Geography
Bulgarian Academy of Sciences, Acad. G.
Bonchev Str., Bl. 3,
1113 Sofia, Bulgaria
kganev@geophys.bas.bg

Slavi Georgiev
Ruse University "Angel Kanchev"
8 Studentska Str.
7017 Ruse, Bulgaria
iivanova@geophys.bas.bg

Ivelina Georgieva
National Institute of Geophysics,
Geodesy and Geography
Bulgarian Academy of Sciences, Acad. G.
Bonchev Str., Bl. 3,
1113 Sofia, Bulgaria
kganev@geophys.bas.bg

Tihomir Gyulov
Ruse University
6 Studentska St
7017 Ruse, Bulgaria
tgulov@uni-ruse.bg

Tsvetan Hristov
Faculty of Mathematics and Informatics
Sofia University "St. Kl. Ohridski"
5 J. Bourchier Blvd.
1164 Sofia, Bulgaria
tsvetan@fmi.uni-sofia.bg

Mario T. Iliev
Faculty of Physics
Sofia University "St. Kliment Ohridski"
5 J. Bourchier Blvd.
1164 Sofia, Bulgaria
ozo@phys.uni-sofia.bg

Oleg Iliev
Fraunhofer Institute for
Industrial Mathematics
oleg.iliev@itwm.fraunhofer.de

Pavel Iliev
Institute of Mechanics
Bulgarian Academy of Sciences
Acad. G. Bonchev Str.,Bl. 4
1113 Sofia, Bulgaria
piliev@imbm.bas.bg

Milena Ilieva
Institute of Neurobiology
Bulgarian Academy of Sciences
Acad. G. Bonchev Str., Bl. 23
1113 Sofia
mil_ilieva@abv.bg

Nevena Ilieva
Institute of Information and
Communication Technologies
Bulgarian Academy of Sciences
Acad. G. Bonchev Str, Bl. 25A
1113 Sofia, Bulgaria
nevena.ilieva@iict.bas.bg
and
Institute of Mathematics and Informatics
Bulgarian Academy of Sciences
Acad. G. Bonchev Str., Bl. 8
1113 Sofia, Bulgaria

Vladimir Ivanov
National Institute of Geophysics,
Geodesy and Geography
Bulgarian Academy of Sciences, Acad. G. Bonchev Str., Bl. 3,
1113 Sofia, Bulgaria
vivanov@geophys.bas.bg

Miglena Koleva
Ruse University
6 Studentska St
7017 Ruse, Bulgaria
mkoleva@uni-ruse.bg

Vladimir Kotev
Institute of Mechanics
Bulgarian Academy of Sciences
Acad. G. Bonchev Str.,Bl. 4
1113 Sofia, Bulgaria
kotev@imbm.bas.bg

Elena Lilkova
Institute of Information and
Communication Technologies
Bulgarian Academy of Sciences
Acad. G. Bonchev Str., Bl. 25A
1113 Sofia, Bulgaria
elena.lilkova@iict.bas.bg

Svetozar Margenov
Institute of Information and
Communication Technologies
Bulgarian Academy of Sciences
Acad. G. Bonchev Str., Bl. 25A
1113 Sofia, Bulgaria
margenov@parallel.bas.bg

Rachel Menda-Shabat-More
Varna Free University "CHERNORISETS HRABAR"
Yanko Slavchev 84, Chaika Resort
9007 Varna, Bulgaria
rachel.shabat@vfu.bg

Zlatogor Minchev
Institute of Information and
Communication Technologies
Bulgarian Academy of Sciences
Acad. G. Bonchev Str., Bl. 25A
1113 Sofia, Bulgaria
zlatogor.minchev@gmail.com

Maya Neytcheva
Uppsala University
mayaneytcheva@gmail.com

Elena Nikolova
Institute of Mechanics
Bulgarian Academy of Sciences
Acad. G. Bonchev Str.,Bl. 4
1113 Sofia, Bulgaria
elena@imbm.bas.bg

Tzvetan Ostromsky
Institute of Information and
Communication Technologies
Bulgarian Academy of Sciences
Acad. G. Bonchev Str., Bl. 25A
1113 Sofia, Bulgaria
ceco@parallel.bas.bg

Peicho Petkov
Faculty of Physics
Sofia University "St. Kl. Ohridski"
5 J. Bourchier Blvd.
1164 Sofia, Bulgaria
peicho@phys.uni-sofia.bg

Nedyu Popivanov
Institute of Information and
Communication Technologies
Bulgarian Academy of Sciences
Acad. G. Bonchev Str., Bl. 25A
1113 Sofia, Bulgaria
nedyu@yahoo.com

Todor Popov
Faculty of Mathematics and Informatics
Sofia University "St. Kl. Ohridski"
5 J. Bourchier Blvd.
1164 Sofia, Bulgaria
topopover@fmi.uni-sofia.bg

Maria Prodanova
National Institute of Geophysics,
Geodesy and Geography
Bulgarian Academy of Sciences, Acad. G.
Bonchev Str., Bl. 3,
1113 Sofia, Bulgaria
maria.prodanova@meteo.bg

Milan Rashevski
Institute of Mechanics
Bulgarian Academy of Sciences
Acad. G. Bonchev Str.,Bl. 4
1113 Sofia, Bulgaria
mrashevski@gmail.com

Sheeru Shamsi
Keele University, UK, ST5 5BG
s.s.shamsi@keele.ac.uk

Nikolay Sirakov
Department of Mathematics
Texas A&M University-Commerce
Commerce, Texas
Nikolay.Sirakov@tamuc.edu

Angela Slavova
Institute of Mathematics and Informatics
Bulgarian Academy of Sciences
Acad. G. Bonchev Str., Bl. 8
1113 Sofia, Bulgaria
slavova@math.bas.bg

Tsvetelina Stefanova
Ruse University
6 Studentska St
7017 Ruse, Bulgaria
tsveti.stefanov@gmail.com

Dimiter Syrakov
National Institute of Geophysics,
Geodesy and Geography
Bulgarian Academy of Sciences, Acad. G.
Bonchev Str., Bl. 3,
1113 Sofia, Bulgaria
dimiter.syrakov@meteo.bg

Venelin Todorov
Institute of Information and
Communication Technologies
Bulgarian Academy of Sciences
Acad. G. Bonchev Str, Bl. 25A
1113 Sofia, Bulgaria
venelinltodorov@gmail.com
and
Institute of Mathematics and Informatics
Bulgarian Academy of Sciences
Acad. G. Bonchev Str., Bl. 8
1113 Sofia, Bulgaria

Nadezhda Todorova
Institute of Biodiversity and
Ecosystem Research,
Bulgarian Academy of Sciences,
nadeshdahr@gmail.com

Toddor Velev
Institute of Information and
Communication Technologies
Bulgarian Academy of Sciences
Acad. G. Bonchev Str., Bl. 25A
1113 Sofia, Bulgaria
toddorv@gmail.com

Nikolay K. Vitanov
Institute of Mechanics
Bulgarian Academy of Sciences
Acad. G. Bonchev Str.,Bl. 4
1113 Sofia, Bulgaria
vitanov@imbm.bas.bg

Krassimira Vlachkova
Faculty of Mathematics and Informatics
Sofia University "St. Kl. Ohridski"
5 J. Bourchier Blvd.
1164 Sofia, Bulgaria
krassivl@fmi.uni-sofia.bg

Lubin Vulkov
Ruse University
6 Studentska St
7017 Ruse, Bulgaria
lvalkov@uni-ruse.bg

Zhan Zhelev
Institute of Mechanics
Bulgarian Academy of Sciences
Acad. G. Bonchev Str.,Bl. 4
1113 Sofia, Bulgaria
zhelev.zhan@gmail.com

Stela Zhelezova
Institute of Mathematics and Informatics
Bulgarian Academy of Sciences
Acad. G. Bonchev Str., Bl. 8
1113 Sofia, Bulgaria
stela@math.bas.bg